NOAA Technical Memorandum NMFS

DECEMBER 2001

MONTHLY MEAN COASTAL UPWELLING INDICES, WEST COAST OF SOUTH AMERICA 1981 TO 2000: TRENDS AND RELATIONSHIPS

Jerrold G. Norton
Franklin B. Schwing
Mark H. Pickett
David Husby
Christopher S. Moore

NOAA-TM-NMFS-SWFSC-316

U.S. DEPARTMENT OF COMMERCE
National Oceanic and Atmospheric Administration
National Marine Fisheries Service
Southwest Fisheries Science Center

The National Oceanic and Atmospheric Administration (NOAA), organized in 1970, has evolved into an agency which establishes national policies and manages and conserves our oceanic, coastal, and atmospheric resources. An organizational element within NOAA, the Office of Fisheries is responsible for fisheries policy and the direction of the National Marine Fisheries Service (NMFS).

In addition to its formal publications, the NMFS uses the NOAA Technical Memorandum series to issue informal scientific and technical publications when complete formal review and editorial processing are not appropriate or feasible. Documents within this series, however, reflect sound professional work and may be referenced in the formal scientific and technical literature.

NOAA Technical Memorandum NMFS
This TM series is used for documentation and timely communication of preliminary results, interim reports, or special purpose information. The TMs have not received complete formal review, editorial control, or detailed editing.

DECEMBER 2001

MONTHLY MEAN COASTAL UPWELLING INDICES, WEST COAST OF SOUTH AMERICA 1981 TO 2000: TRENDS AND RELATIONSHIPS

Jerrold G. Norton[1], Franklin B. Schwing[1],
Mark H. Pickett[1], David Husby[2], and Christopher S. Moore[1]

[1]National Oceanic and Atmospheric Administration
National Marine Fisheries Service
Southwest Fisheries Science Center
Pacific Fisheries Environmental Laboratory
1352 Lighthouse Avenue
Pacific Grove, California 93950

[2]Joint Institute for Marine and Atmospheric Research (JIMAR)
University of Hawaii at Manoa
1000 Pope Road
Honolulu, HI 96822

NOAA-TM-NMFS-SWFSC-316

U.S. DEPARTMENT OF COMMERCE
Donald L. Evans, Secretary
National Oceanic and Atmospheric Administration
Conrad C. Lautenbacher, Jr., Under Secretary for Oceans and Atmosphere
National Marine Fisheries Service
William T. Hogarth, Assistant Administrator for Fisheries

CONTENTS

ABSTRACT

The Pacific Fisheries Environmental Laboratory (PFEL) upwelling index provides continuous proxy time series of coastal ocean processes which are difficult to measure directly and are infrequently available for the study of surface layer physical and biological ocean dynamics. The PFEL Upwelling Index (UI) is derived from analyzed pressure fields using planetary boundary layer theory and the geostrophic wind approximation to derive inferences about momentum transport from the wind to the sea surface layer. The UI values for the period January 1981 through December 2000 are analyzed for the highly productive upwelling systems off the coasts of Peru and Chile. These data have been extracted for two sets of 11 locations from 15° to 45°S. Large-scale characteristics of these time series include: 1) Highest UI values are in the austral spring and summer; 2) Maximum UI occurs earlier in the year at lower latitudes; 3) Mean UI is negative for short periods during austral winter; 4) Austral spring and summer UI increases from 45° to 30°S; 5) The largest UI values are found north and south of 21°S; 6) Variation in UI is dependent on computation point distance from shore and adjacent land topography; 7) Interannual variation increases three fold from south to north; 8) North of 24°S, greatest interannual variation occurs during the June to December period; 9) Interannual variability in UI approaches the magnitude of seasonal variability north of 24°S; and 10) Negative UI anomaly at 15°S, 18°S and 21°S increases in magnitude after 1994 and during El Niño-Southern Oscillation periods. The UI for the west coast of South America reflects physical environmental changes expected to influence temporally and spatially coincident ecosystems.

INTRODUCTION

Since the early 1970's, the Pacific Fisheries Environmental Laboratory (PFEL) has produced an index of wind-forced offshore Ekman transport along the west coast of North America (Bakun, 1973). These indices are calculated from surface atmospheric pressure fields produced by the U. S. Navy Fleet Numerical Meteorology and Oceanography Center (Clancy, 1992; Rosmond, 1992). Subsequent development by Bakun (1975) and others allows the PFEL Upwelling Index (UI) and associated atmospheric parameters to be calculated for any location in the world's oceans (Mason and Bakun, 1986; Schwing et al., 1996). These products are regularly distributed to users worldwide, including scientific researchers, resource managers, private entrepreneurs and sportsmen.

The frictional stress of equatorward wind on the ocean causes water in the surface layer to move away from the west coast of North and South America (Sverdrup et al., 1942; Wooster and Reid, 1963; Smith, 1968; Bakun, 1975). The offshore moving surface water, referred to as Ekman transport, is replaced by water which upwells along the coast from depths of 10 to more than 60 m, depending on vertical patterns of ocean stability (Figure 1).

Upwelled water is typically cooler than the surface water displaced offshore and frequently has much greater concentrations of dissolved nutrients if the upwelled water is from below the euphotic zone (Wooster and Reid, 1963; Smith, 1968; Thomas et al., 1994; Strub et al., 1998). These nutrients are essential in sustaining

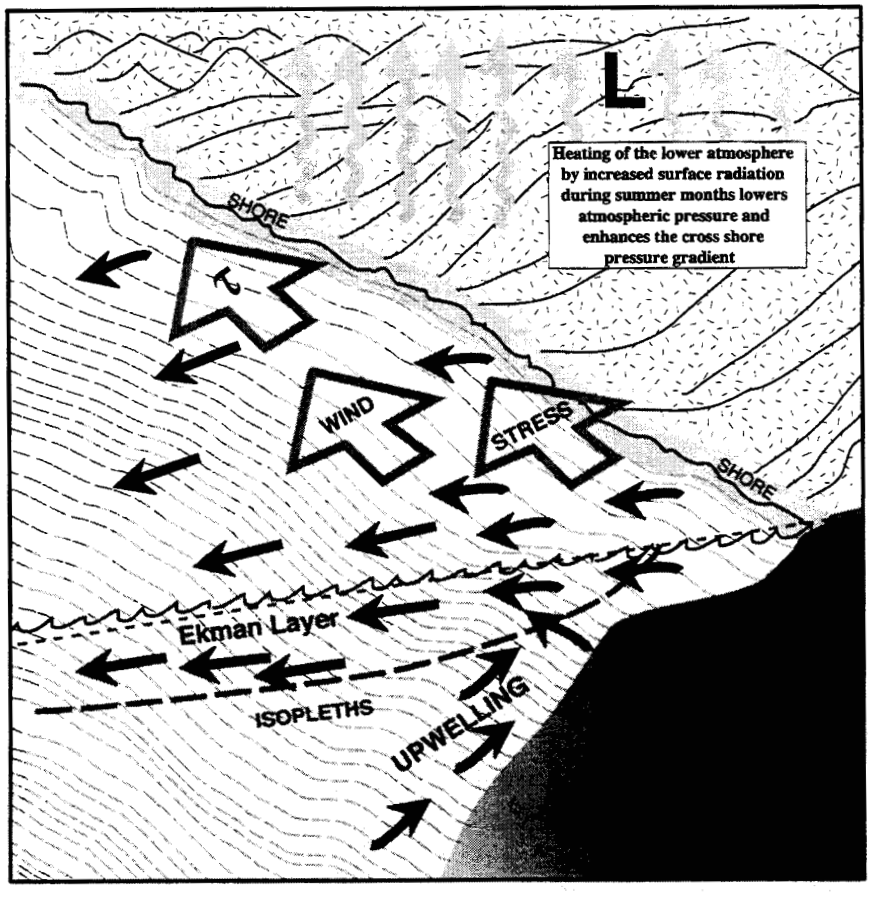

Figure 1. Diagram of the effects of winds stress (open arrows) on coastal upwelling and offshore Ekman transport (black arrows) along the west coast of Peru and Chile. Mean winds blow from south to north enhancing coastal upwelling of subsurface water. Upwelling leads to an on-offshore pressure gradient, with lower sea level shoreward compared to level surface (short dash). Gray, wavy, vertical arrows suggest surface heating over land and low pressure typical of the austral summer. Equatorward wind stress occurs at the eastern limb of the subtropical high atmospheric pressure system.

primary production and higher trophic levels (Peterson and Miller, 1977; Traganza et al., 1981; Thomas et al., 1994). For this reason, upwelling ecosystems are highly productive (Wooster and Reid, 1963; Ryther, 1969). Primary production commonly exceeds 2 g carbon per m^2 per day in each of the major upwelling regions. Fish production within the eastern South Pacific, eastern South Atlantic and California Current upwelling regions may each exceed a million metric tons per year (Mann and Lazier, 1996). Upwelling indices have been correlated with condition factors, recruitment and abundance of commercially important fish throughout the world (Ryther, 1969; Parrish et al., 1981; Norton, 1987; Cury et al., 1995; Ainley et al., 1994; Thomas et al., 1994; VenTresca et al., 1995; Durand et al., 1998).

Each month PFEL generates synoptic scale (100 to 1000 km) wind forcing indices which include the UI for the Peru-Chile Current and the California Current upwelling ecosystems. The Peru-Chile UI is currently available in the Appendix and via the Internet at:

http://www.pfeg.noaa.gov

PFEL UI calculations are based on Ekman's (1905) theoretical derivations of steady mass transport due to the momentum balance between Coriolis acceleration acting on the current and the divergence of the wind stress, assuming homogeneity, uniform wind, and steady state conditions. The mass transport of surface water due to wind stress is 90° to the left (right) of the wind when the wind is pressing at an observer's back in the Southern (Northern) Hemisphere. Ekman mass transport is given by wind stress divided by the Coriolis parameter (τ / f). The depth to which an appreciable amount of offshore transport occurs is termed the surface Ekman layer and is generally 10 to more than 60 m deep depending on surface wind speed and direction, latitude, and ocean stratification (Price and Sundermeyer, 1999). Since $f = 2\theta \sin(\phi)$, where θ is the angular rotation of the earth and ϕ the latitude, f increases more than two fold from 21° to 45°S. Consequently, equatorward winds of equal magnitude will result in nearly twice as much offshore Ekman transport at 20°S, off Peru, as at 45°S, off southern Chile.

Wooster and Reid (1963) used the offshore component of surface Ekman transport as an "index of upwelling" that describes a portion of the seasonal variation in temperature and dissolved nutrients in the coastal California Current. The magnitude of the offshore component is taken as an index of the amount of water upwelled from the base of the Ekman layer. Offshore Ekman transport in metric tons/second/100 meters of coastline is the PFEL upwelling index and assigned positive values. Negative values imply downwelling, the onshore advection of surface waters accompanied by a downward displacement near the coastal boundary.

In accordance with the primary goals of PFEL to provide meaningful physical environmental data to the fisheries research community, UI computations have been made from the monthly mean pressure fields for 22 locations in major upwelling systems along the west coast of South America: 11 Coastal locations, within 100 km of the local coastline; and 11 Offshore locations, 100 to 300 km offshore (Figure 2). These locations were chosen to illustrate the effects of the continental boundary on UI computations.

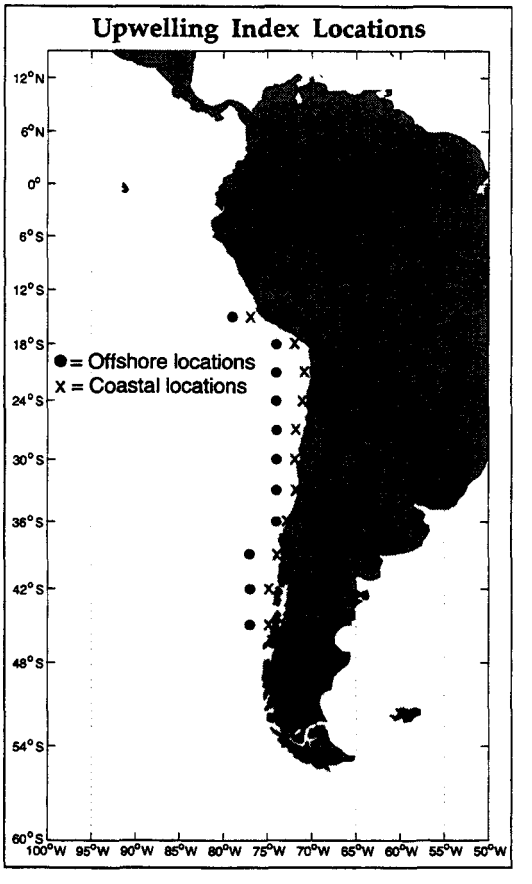

Figure 2. Upwelling computation locations off the west coast of South America. The Offshore locations are 100 to 300 km offshore. The Coastal locations are closer than 100 km.

COMPUTATIONS AND ANALYSES

Global gridded sea level atmospheric pressure fields became available from Fleet Numerical Meteorology and Oceanography Center (FNMOC) in 1981. These 2.5° x 2.5° (73 x 144 global spherical projection) grids are produced at 6 hourly intervals from incoming observations, forecasts and analyses (Clancy, 1992; Rosmond, 1992). Upwelling Index calculations were made after extrapolating the 2.5° x 2.5° pressure fields to a 3° computation grid length on a spherical coordinate system using a Bessel 16-point central difference formula. This maintained the 3° x 3° (Figure 3, dark shading) conventions used in previous UI calculations (Bakun, 1973; Bakun, 1975). In November 1996, the 2.5° x 2.5° fields were replaced with 1° x 1° (360 x 181 global spherical) grids. Computations of UI from November 1996 to the present are based on this finer gridded data; however, upwelling indices continue to be calculated from a 3° computational mesh wherein each point contributing to the final computation is derived from Bessel interpolation of the 16-point grid of the monthly mean sea level pressure field (Figure 3).

In comparing mean sea level atmospheric pressure from the 1° x 1° fields to mean sea level atmospheric pressure from the 2.5° x 2.5° fields, it was found that the mean fields were nearly identical and generally agree to within ± 0.1 millibar. However, differences are expected in the UI, because computations from the 2.5° x 2.5° fields smooth the physical gradients more than computations from the 1° x 1° fields (Figure 3).

For this report, monthly mean upwelling indices have been produced for 22 locations from 15°S to 45°S at 50 to 500 km from shore (Figure 2). This range extends from tropical to cool temperate climates. The UI computation, reviewed below, follows the procedures used in all previous PFEL UI computations (Bakun, 1973, 1975; Mason and Bakun, 1986; Schwing et al., 1996).

Derivatives of the sea level atmospheric pressure, P, at each computation point (Figure 3, dark shading, center) are estimated by taking the difference in pressure between the grid points to either side and dividing by the 6° angular mesh length,

$$\partial P/\partial \phi \approx (P_{\lambda,\phi+h} - P_{\lambda,\phi-h})(2h)^{-1} \qquad (1)$$

$$\partial P/\partial \lambda \approx (P_{\lambda+h,\phi} - P_{\lambda-h,\phi})(2h)^{-1} \qquad (2)$$

where ϕ and λ are the north and east angular coordinates, respectively, and h is the 3° mesh length in radians (Figure 3).

The east (u_g) and north (v_g) components of the geostrophic wind are:

$$u_g = -(f\rho_a R)^{-1}\ \partial P/\partial \phi \qquad (3)$$

$$v_g = (f\rho_a R \cos\phi)^{-1}\ \partial P/\partial \lambda \qquad (4)$$

where f is the Coriolis parameter (negative for Southern Hemisphere), ρ_a is the density of air (assumed constant at 1.22 kg/m^3), and **R** is the mean radius of the Earth (6371.2 km).

Assuming no friction, the geostrophic wind is parallel to local isobars, with low pressure to the right in the Southern Hemisphere; i.e., wind circulates clockwise (cyclonically) around Southern Hemisphere areas of low pressure. To approximate frictional effects, the geostrophic wind at the sea surface is estimated by rotating the geostrophic wind 15° to the right and reducing its magnitude by 30%.

Sea surface wind stress is calculated from the geostrophic wind using the square-law formula:

$$\vec{\tau} = \rho_a C_d |\vec{v}| \vec{v} \qquad (5)$$

where $\vec{\tau}$ is the wind stress vector, C_d is an empirical drag coefficient and $\vec{v}$ is the estimated wind vector near the sea surface with magnitude $|\vec{v}|$. The value used to calculate upwelling from the monthly-mean fields is $C_d = 0.0026$ (Bakun, 1973; Davidson, 1974; Nelson, 1977, Thonpson, et al., 1983). A $C_d = 0.0013$ was used by Bakun (1975) for the calculation of UI from six-hourly FNMOC pressure fields.

Ekman transport, $\vec{M}$, is calculated using:

$$\vec{M} = (\vec{\tau} \times \vec{k}) f^{-1} \qquad (6)$$

where $\vec{k}$ is the unit vector directed vertically upward.

The sign of the offshore component of Ekman transport, $M_x = \tau_y / f$, where x is normal and y parallel to the local coastline orientation, is then

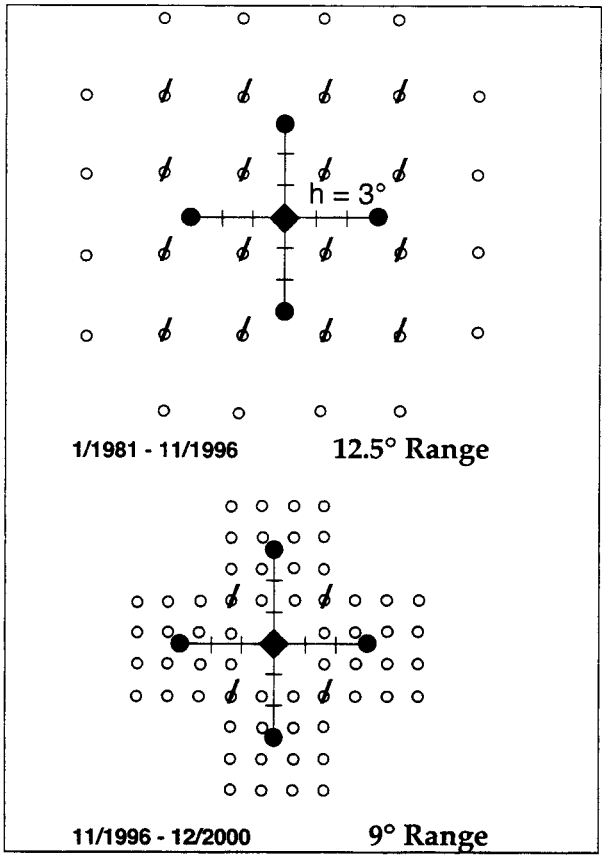

Figure 3. For all Upwelling Index computations, the specified point is the center point (square) of the darkly shaded 6° x 6° array. The darkly shaded circles show derived points that are used to compute upwelling index at the central location. Derived computation points are computed from the 16 closest data grid points (smaller circles). The upper diagram shows the range of grid points from which the computation points are calculated when the source global data grid has 2.5° x 2.5° length and the lower panel shows grid spacing for the 1° x 1° data grid currently used. Diagonals mark data grid points that are used more than once in the overall computation.

reversed to reflect that negative (offshore) Ekman transport, in Equations 3 through 6, leads to positive vertical transport (upwelling), and positive, in Equations 3 through 6, (onshore) Ekman transport leads to negative vertical transport (downwelling). UI values are expressed in units of metric tons (cubic meters) per second per 100 meters of coastline (t/s/100m).

The UI is most generally interpreted as an index of upwelling occurring along 100 - 500 km of coastline, rather than an indicator of upwelling at precise computation points. There is generally considerable correlation between points computed at 3° intervals along the coast (Schwing et al., 1996; and below).

Biharmonic analyses (Lynn, 1967) for each of the 22 Peru-Chile Current locations are presented as graphs for selected Coastal and Offshore locations. These graphs show the biharmonic fit to the computed data within an envelope of ±1.0 standard error (Schwing et al., 1996). Biharmonic analysis fits the UI for time interval, **t**, at a particular computation point to equations of the form

$$\mathbf{UI(t) = A0 + A1cos(2\Pi t) + B1sin(2\Pi t) + A2cos(4\Pi t) + B2sin(4\Pi t)} \quad (7)$$

There will be an annual harmonic, unless there is no variation in the input data. If the annual cycles of input data do not form a perfectly symmetrical annual sinusoid, then there will be a semi-annual harmonic.

RESULTS

Mean annual cycles of UI for the Coastal and Offshore series of computation points (Figure 4) are in qualitative agreement with accepted climatology for the coasts of Peru and Chile (Bakun and Nelson, 1991; Hill et al., 1998). The UI diagnosis of a robust upwelling system off Peru that is influenced by equatorial events agrees with the observations of Smith et al. (1971), Richards (1981), Thomas et al. (1994); Strub et al. (1998), Hill et al., (1998), and Blanco et al., (2001). The northward alongshore wind stress minimum at 20°S shown by Hill et al. (1998) in data from the European Center for Medium-Range Forecasts (ECMWF) is coincident with the UI minimum at 21° and 24°S (Figures 4 and 5). A southern UI maximum near 30°S during austral summer is in agreement with the observations by Maeda and Kishimoto (1970) and Hill et al. (1998). Austral winter UI minima from 35° to 45°S (Figure 4) also agree with ECMWF wind stress data (Hill et al., 1998).

There are quantitative differences from results based on daily ECMWF wind fields. South of 20°S, UI values for the Coastal computation set may be inflated by a factor of 1.1 - 2.0 (see DISCUSSION and CONCLUSIONS). Maxima and minima may be shifted 1° to 3° equatorward in UI climatologies (e.g. Figure 4). This shift has been described for the west coast of North America by Bakun (1973,1975).

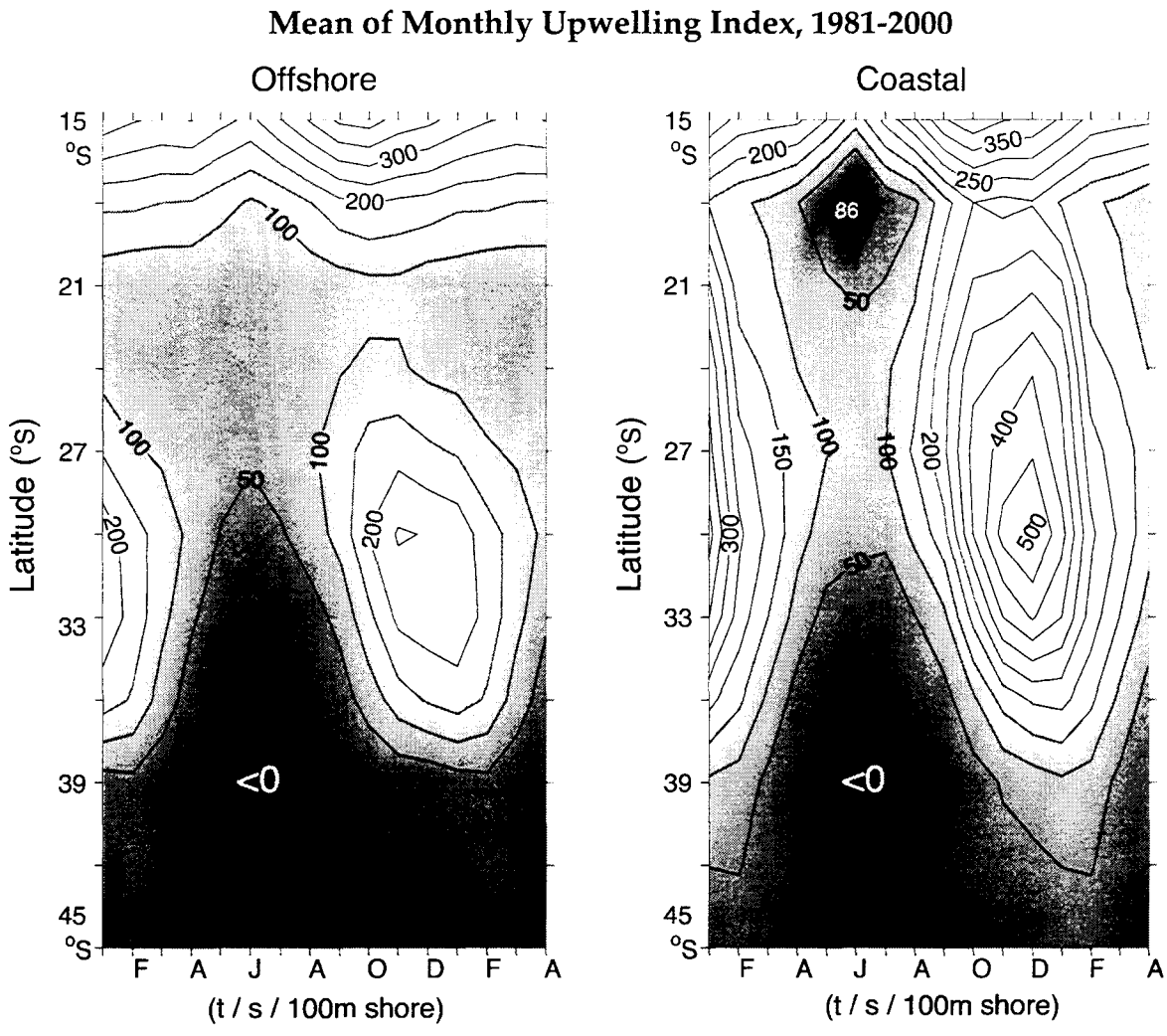

Figure 4. Overall mean (1981-2000) annual cycle of PFEL Upwelling Index (UI) summarized for the Offshore and Coastal locations 15°-45° S off the west coast of South America. The range of means is from -86 to 512 t/s/100m of coastal length. The abscissa is month, with January at the left. The first four months of the year are repeated on the right. Lighter shading gives larger Upwelling Index values. Ordinates give latitude.

The magnitude of mean upwelling at Offshore and Coastal locations is similar at 15°S and 18°S, but there is greater amplitude in the annual cycle at the Coastal locations. Negative UI is found at 18°S for the Coastal points, but Offshore UI remains at 50 t/s/100m or above throughout the year. The Coastal mean at 18°S has a June minimum of less than -80 t/s/100m. For the Offshore set, the northern minimum in UI also occurs in June, but remains positive and is displaced poleward (Figure 4).

Seasonal patterns are similar for Coastal and Offshore sets at mid-latitude (24° to 39°S) but the means for the Coastal computation set show higher amplitude seasonal cycles (Figures 4, 5, 6 and 7). The overall means of more than 400 t/s/100m in Coastal UI during November, December and January are twice those calculated for the Offshore points. These Coastal values are one-third to two-thirds greater than the overall means calculated by Schwing *et al.* (1996) for similar latitudes off the west coast of North America. Mid-latitude UI maxima are in the eleventh and twelfth months for Coastal and Offshore locations. South of 39°S, the annual amplitude is similar for Coastal and Offshore computation sets, with longer seasons of positive upwelling computed for the Coastal locations. Upwelling index maxima occur later in the upwelling season at 33°S than at 15°S in the Offshore and Coastal data sets (Figures 4, 6 and 7).

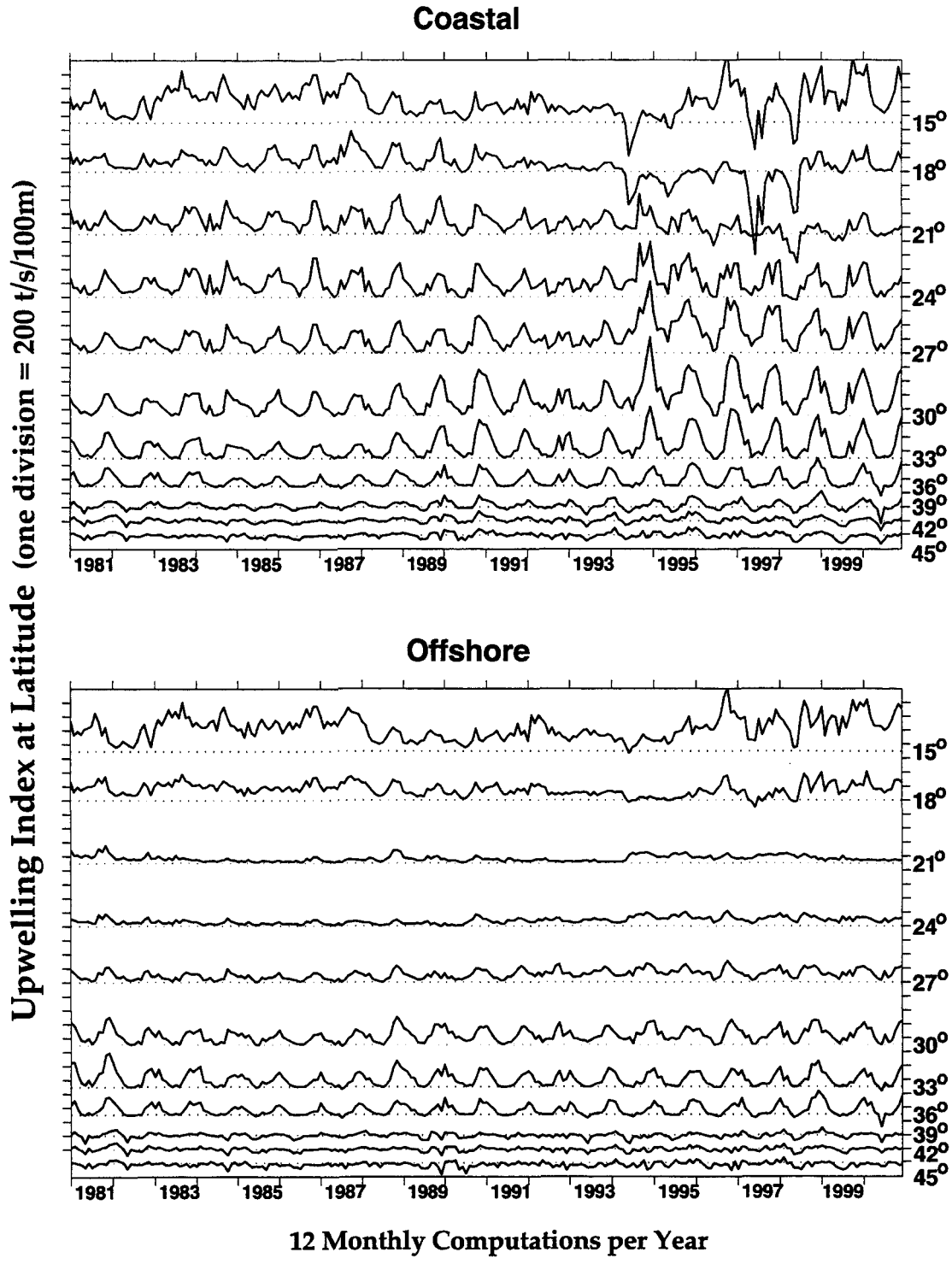

Figure 5. Time series of monthly mean Upwelling Index computed for 11 locations of the Coastal (upper) and Offshore (lower) series. Solid line gives Upwelling Index. Dotted line gives a zero reference. Each vertical division represents 200 t/s/100m of coastline. Lower latitudes are toward the top (right).

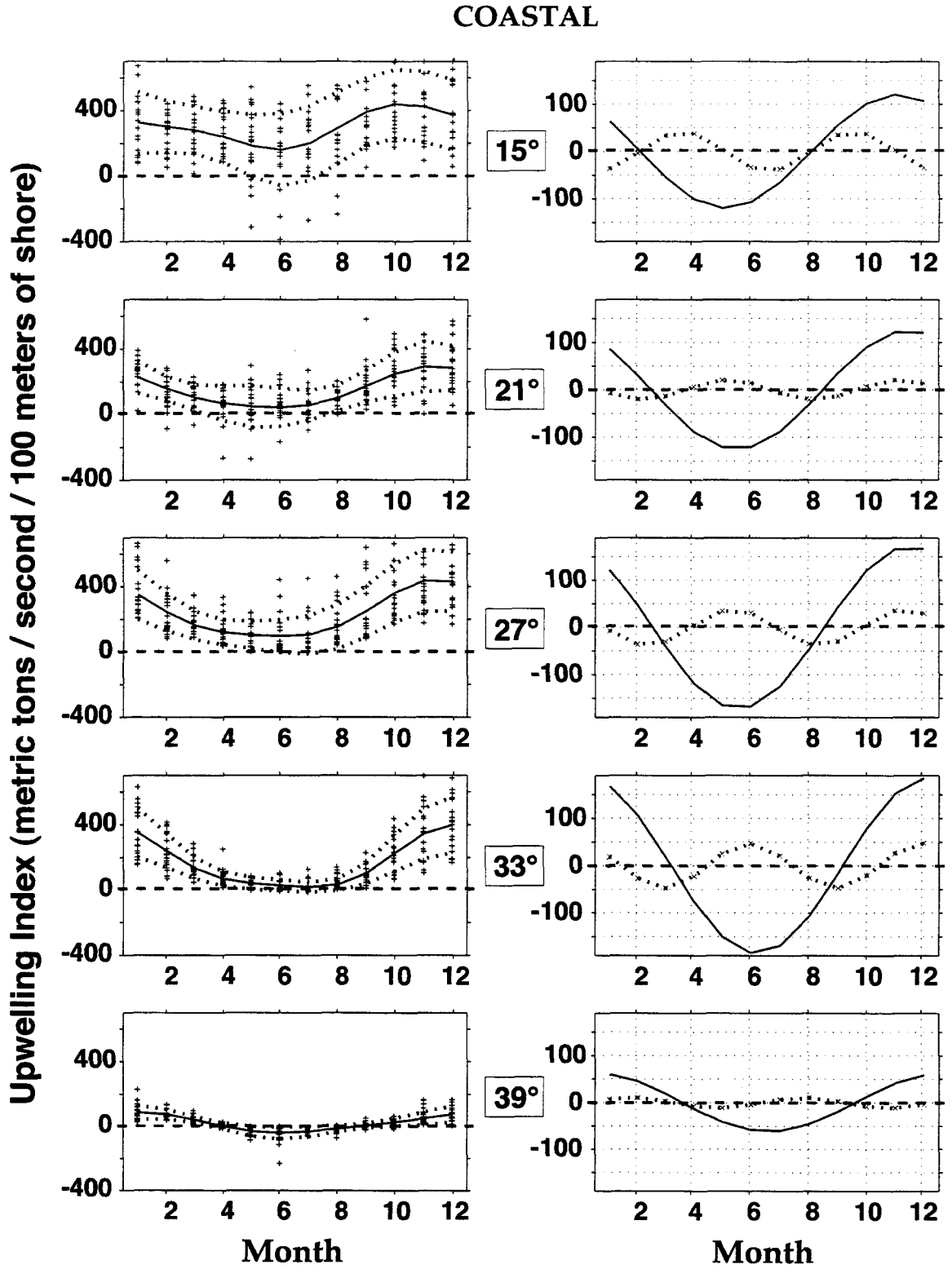

Figure 6. Biharmonic fits to annual and semi-annual cycles within ±1.0 standard error envelopes (dotted) of UI (solid) computed for five locations (center) from the Coastal set of computation points. Symbols show computed UI values of -400 to 600 t/s/100m of coastline. Graphs on the right show least squares fitted harmonics, with mean adjusted to zero. Values are plotted by month, with January on the left. Solid lines show the annual fit and dotted lines show semi-annual fit.

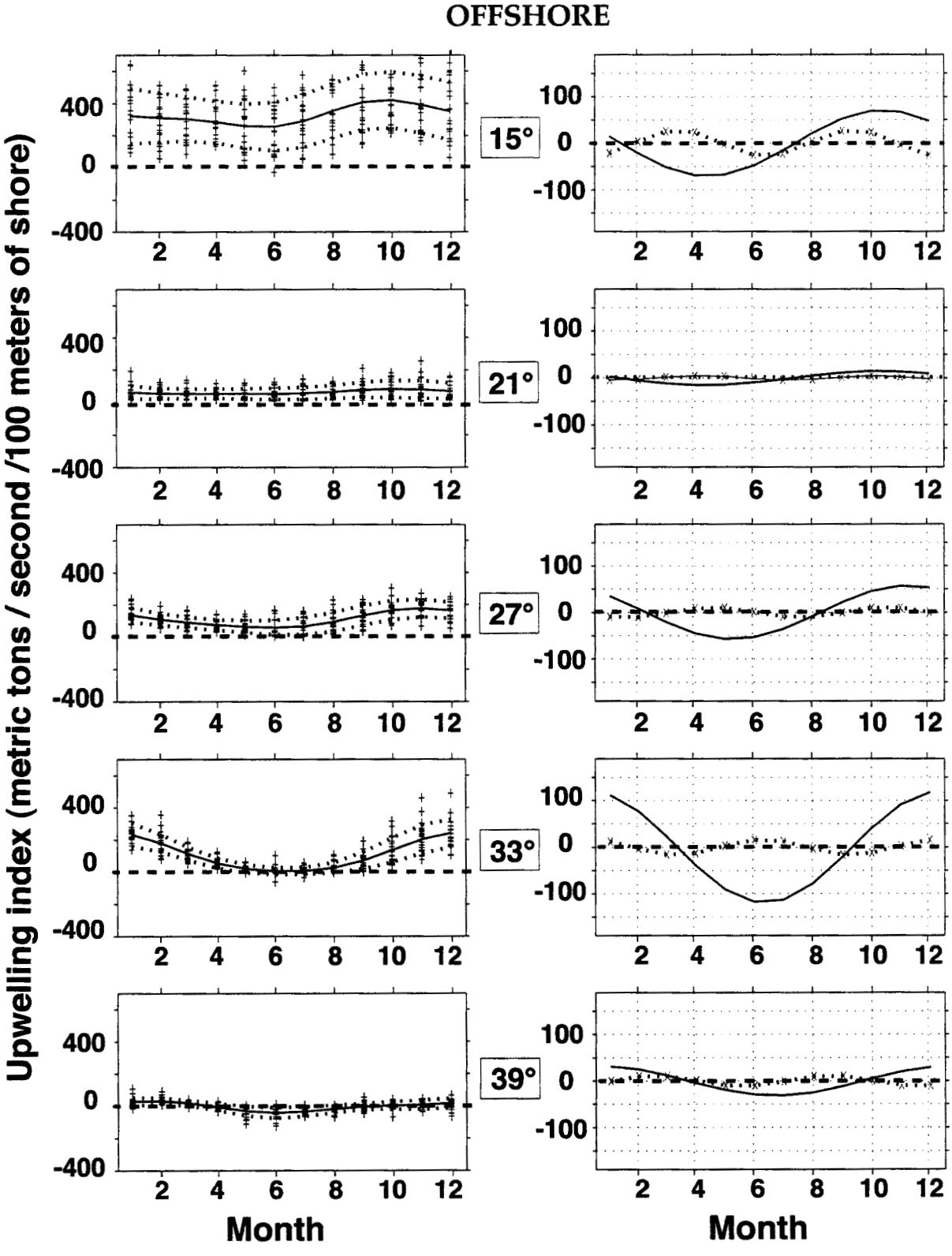

Figure 7. Biharmonic fits to annual and semi-annual cycles within ±1.0 standard error envelopes (dotted) of UI (solid) computed for five locations (center) from the Offshore set of computation points. Symbols show computed UI values of -400 to 600 t/s/100m of coastline. Graphs on the right show least squares fitted harmonics, with mean adjusted to zero. Values are plotted by month, with January on the left. Solid lines show the annual fit and dotted lines show semi-annual fit.

Time series of monthly mean values for all 22 locations are compared in Figure 5. Before 1991, the annual cycle is clear in all 11 Coastal time series. After 1991 the annual cycle becomes less distinct at 21°S and northward (upper panel). South of 21°S, the annual cycle remains distinct through the 1981 to 1999 period, but variability increases during the 1990 to 2000 period at the Coastal locations. Before about 1993, Coastal UI time series can be divided into a northern group, 15° to 33°S, with robust annual cycles and a southern group, 36° to 45°S, with weak and variable annual cycles. After 1993, the annual cycle becomes less dominant at 21°S and northward, but more dominant at 24° to 33°S. Increased annual cycle amplitude at the 24° to 33°S Coastal stations after 1993 is predominately due to increased UI during the austral summer (Figure 5).

The annual cycle and other periodicities have lower amplitudes in the Offshore UI time series (Figure 5, lower panel). Distinct annual cycles are evident from 27°S southward to 39°S. Variability in monthly mean values is low for the 21° and 24°S Offshore computation points. Amplitudes of dominant cycles are an order of magnitude greater at the Coastal 21° and 24°S points than at the corresponding Offshore points. The 21° and 24°S points are immediately south of the bight that extends from 15° to 22°S and includes the ocean south of Peru between 70° and 75°W. In addition, the Atacama Desert, adjacent to the coast between 18° and 25°S, may influence sea level pressure distribution in this area that appears to be a null between areas of different seasonal tendency (Figure 5, lower panel).

Time series from the Offshore set may be divided into four groups according to latitude. The tropical set of high interannual variability is located at 15° and 18°S and the tropical set of low variability series is located at 21° and 24°S. Farther south the temperate computation points with more robust annual cycle is located at 30° to 36°S, and the temperate group of low variability is located at 39° to 45°S.

The 15° and 18°S time series in both Coastal and Offshore sets appear erratic after November 1996 when the sea level pressure grid was changed from 2.5° x 2.5° to 1° x 1° (see COMPUTATIONS and ANALYSES). However, it is not completely clear that the change in variability after November 1996 is related to FNMOC data changes because there is at least visual continuity in the more southern stations before and after November 1996 and the variability in the 1994 to 1995 annual cycles is similar, but of lower magnitude, than that found in the 1997 to 2000 annual cycles (Figure 5).

Biharmonic analysis focuses on annual and semi-annual harmonics of the 1981 to 2000 ensemble of monthly means at each computation point. The shape of the mean annual cycle as shown by the computed UI time series is fitted to a biharmonic equation by least-squares techniques. This fit determines the amplitude and phasing of the two harmonics. The biharmonic fit, a ±1.0 standard error envelope, and the original computed UI points are shown in the left panels of Figures 6 and 7. The annual and semi-annual harmonic components are shown for five representative latitudes from 15° to 39°S (Figures 6 and 7). Both annual and semi-annual harmonic components have higher amplitudes at the Coastal points suggesting more robust annual cycles with considerable interannual variability. Partial coincidence of two harmonic maxima in the later months of the year show that mean seasonal maxima UI appear earlier at the northern computation locations.

Coastal and Offshore stations at 15°S are only 108 km (1° longitude) apart and are the most similar in biharmonic decomposition when Coastal and Offshore locations are compared. However, the Coastal 15°S location has higher seasonal amplitude and higher interannual variability. The difference in interannual variability between Coastal and Offshore stations at 15°S is also apparent in Figure 5.

The correlation patterns of UI anomaly series shown in Table 1 suggest that the closest computation points are frequently the most closely related on interannual scales (compare to Figure 2). Computation points south of 24°S are most closely correlated with one another for both computation sets. Points over 1000 km distant are seldom highly correlated (Table 1).

The Coastal and Offshore time series at 15°S are the most highly correlated of the tropical points (Table 1, lower left). At 30° to 45°S, a closer relationship between Coastal and Offshore points is found. The highest correlation coefficient is where the Offshore and Coastal points are separated by 90 km at 36°S. However, the correlation of the 36°S Offshore and the 39°S Coastal locations is also high.

	Coastal											Offshore									
S Lat. x	15x	18x	21x	24x	27x	30x	33x	36x	39x	42x	45x	15x	18x	21x	24x	27x	30x	33x	36x	39x	42x
E Long.	76	72	71	71	72	72	72	73	74	75	75	77	74	74	74	74	74	74	74	77	77
Coastal																					
18x72	0.63																				
21x71		0.48																			
24x71			0.6																		
27x72		-0.4		0.77																	
30x72		-0.3		0.59	0.92																
33x72		-0.3		0.4	0.75	0.92															
36x73					0.39	0.54	0.76														
39x74							0.37	0.75													
42x75						0.21	0.34	0.57	0.79												
45x75							0.21	0.4	0.63	0.9											
Offshore																					
15x77	0.91	0.34																			
18x74	0.82	0.73	0.25		-0.2	-0.2	-0.2					0.75									
21x74	-0.2	-0.3	0.04	0.3	0.39	0.3	0.3	0.25													
24x74		-0.4	-0.2	0.42	0.72	0.62	0.54	0.39						0.64							
27x74		-0.3		0.39	0.68	0.62	0.56	0.45	0.13	0.15				0.45	0.87						
30x74				0.23	0.45	0.53	0.64	0.67	0.31	0.27				0.49	0.56	0.77					
33x74							0.38	0.71	0.45	0.39	0.24			0.45	0.25	0.38	0.79				
36x74							0.43	0.89	0.81	0.56	0.42			0.22	0.23	0.31	0.6	0.8			
39x77								0.24	0.66	0.64	0.59		0.22					0.32	0.49		
42x77								0.25	0.53	0.76	0.8							0.34	0.42	0.86	
45x77									0.32	0.6	0.82								0.21	0.61	0.86

Table 1. Spatial patterns of correlation in time series of Upwelling Index (UI) anomaly for the 22 computation locations. Correlation coefficients showing intercorrelation of the Coastal locations are upper left and coefficients for the intercorrelation of the Offshore stations are at the lower right. Coefficients for the correlation of the Coastal set with the Offshore set are lower left. Coefficients between -0.2 and 0.2 are omitted. Coefficients greater than |0.6| are underlined to show patterns of association. Nominally, coefficients greater than |0.25| will occur by chance less than one percent of the time (240 monthly samples, 220 table entries).

Relatively low correlation between adjacent points is found between 18°S and 24°S.

Interannual variability was examined in two sets of 22 panels, one set for the Coastal and one set for the Offshore computation locations (Figures 8 and 9). In each set, the first two panels show the mean annual cycle, simplified from Figure 4, and the standard deviation of the 1981 to 2000 monthly mean values. The next 20 panels show UI anomaly on a month by latitude grid for the 1981 to 2000 period.

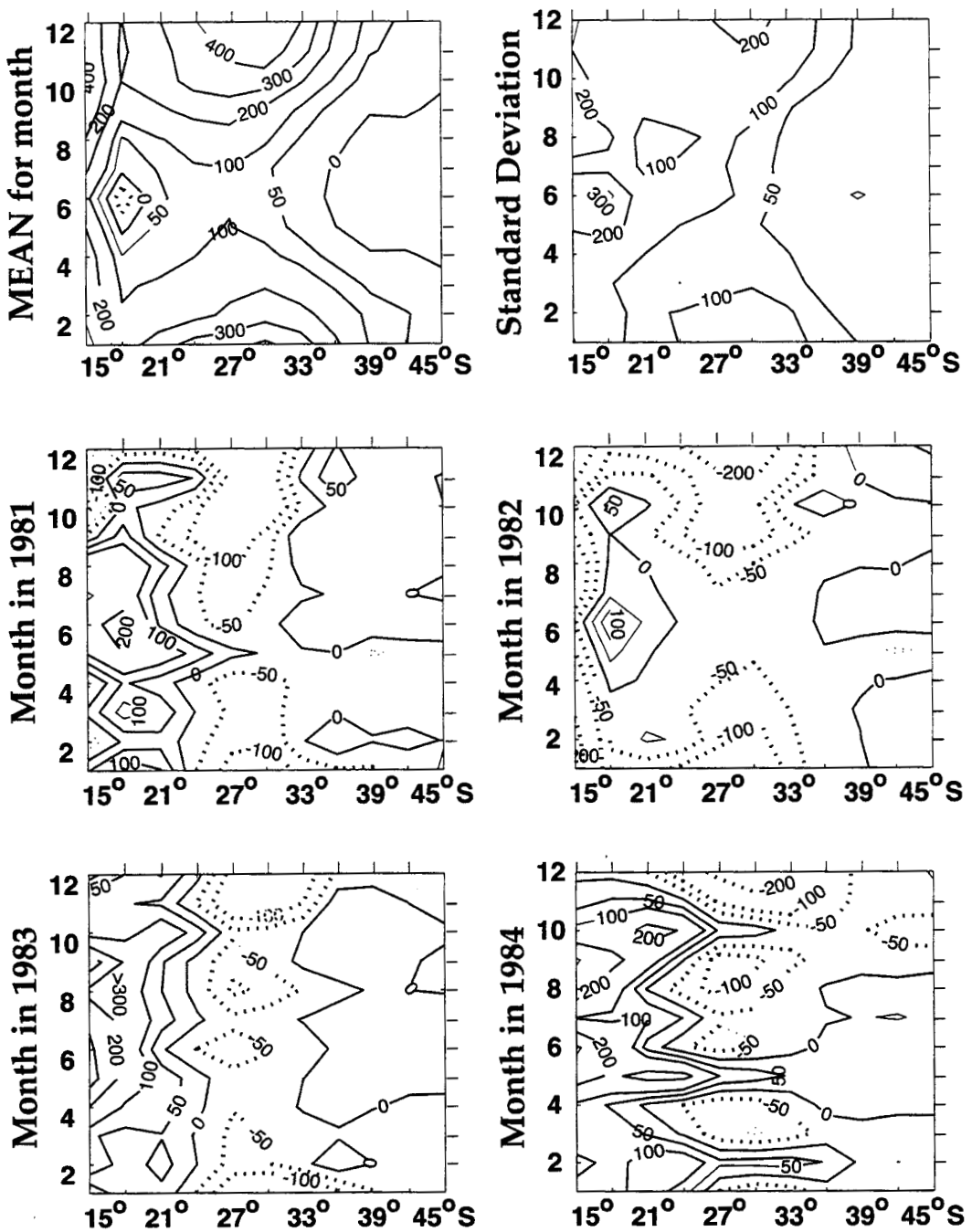

Figure 8. Mean annual cycles are contoured in the upper left panel for the Coastal locations. The overall standard deviation of monthly mean Upwelling Index is upper right. The lower 20 panels show annual distribution of anomaly for the years 1981 to 2000. Contours are 0, 50, 100, 200 and 300 t/s/100m of coastline. Dotted contours show negative anomaly compared to the overall mean. Selected extreme values are indicated. Months are on the ordinate with January at the lower left. Abscissas show latitude from 15° to 45° S.

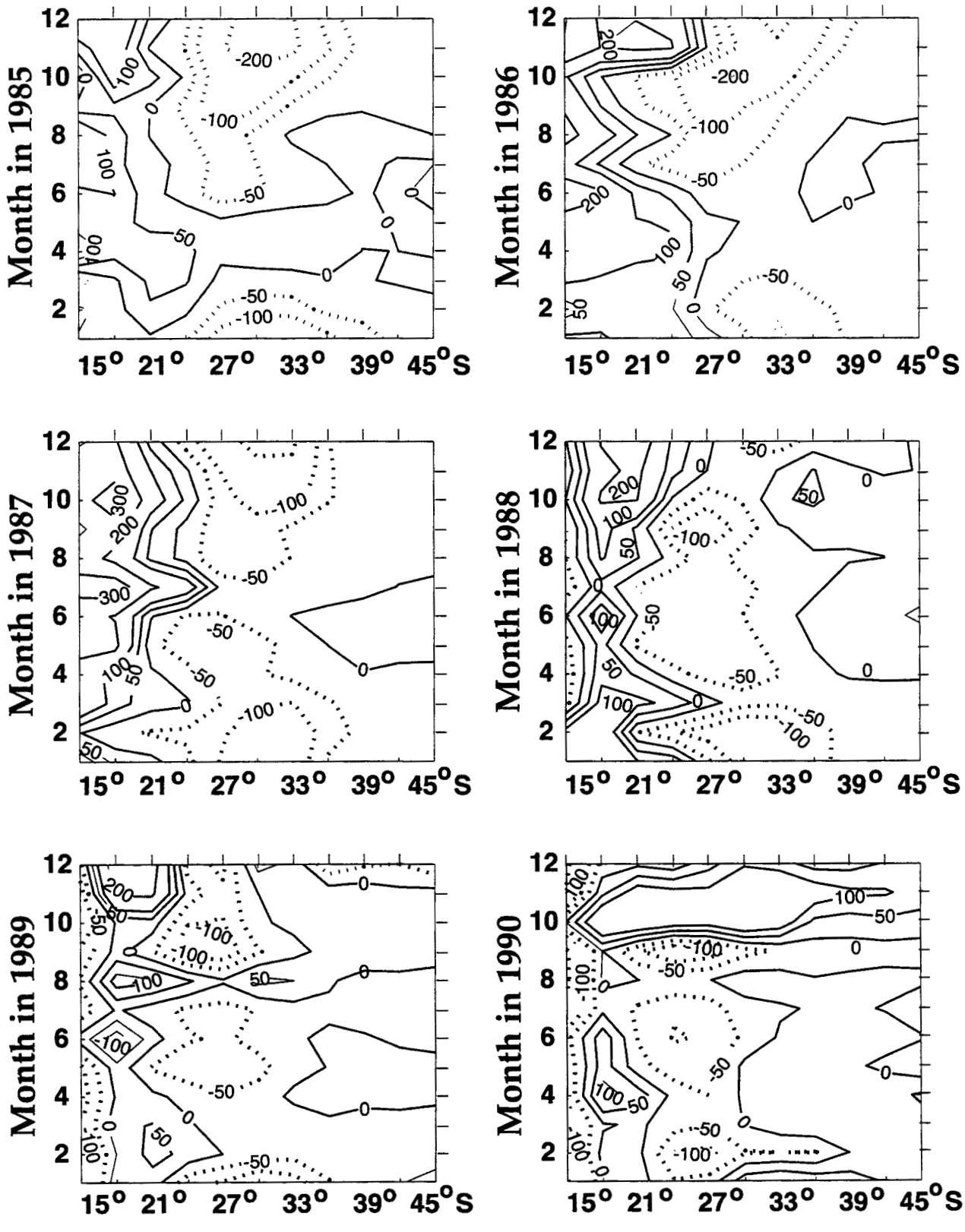

Figure 8 (continued). Contours are 0, 50, 100, 200 and 300 t/s/100m of coastline. Dotted contours show negative anomaly compared to the overall mean. Selected extreme values are indicated. Months are on the ordinate with January at the lower left. Abscissas show latitude from 15° to 45° S.

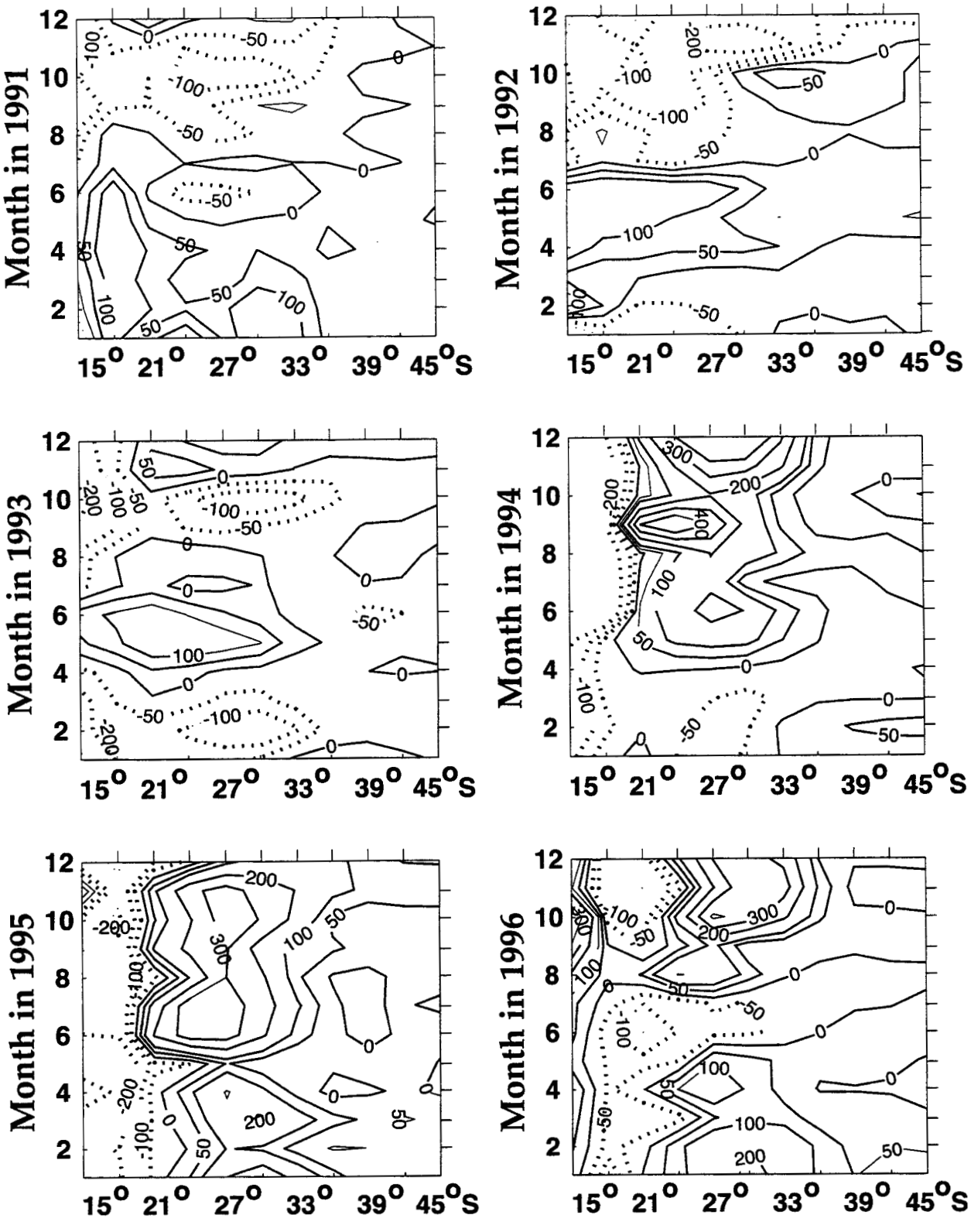

Figure 8 (continued). Contours are 0, 50, 100, 200 and 300 t/s/100m of coastline. Dotted contours show negative anomaly compared to the overall mean. Selected extreme values are indicated. Months are on the ordinate with January at the lower left. Abscissas show latitude from 15° to 45° S.

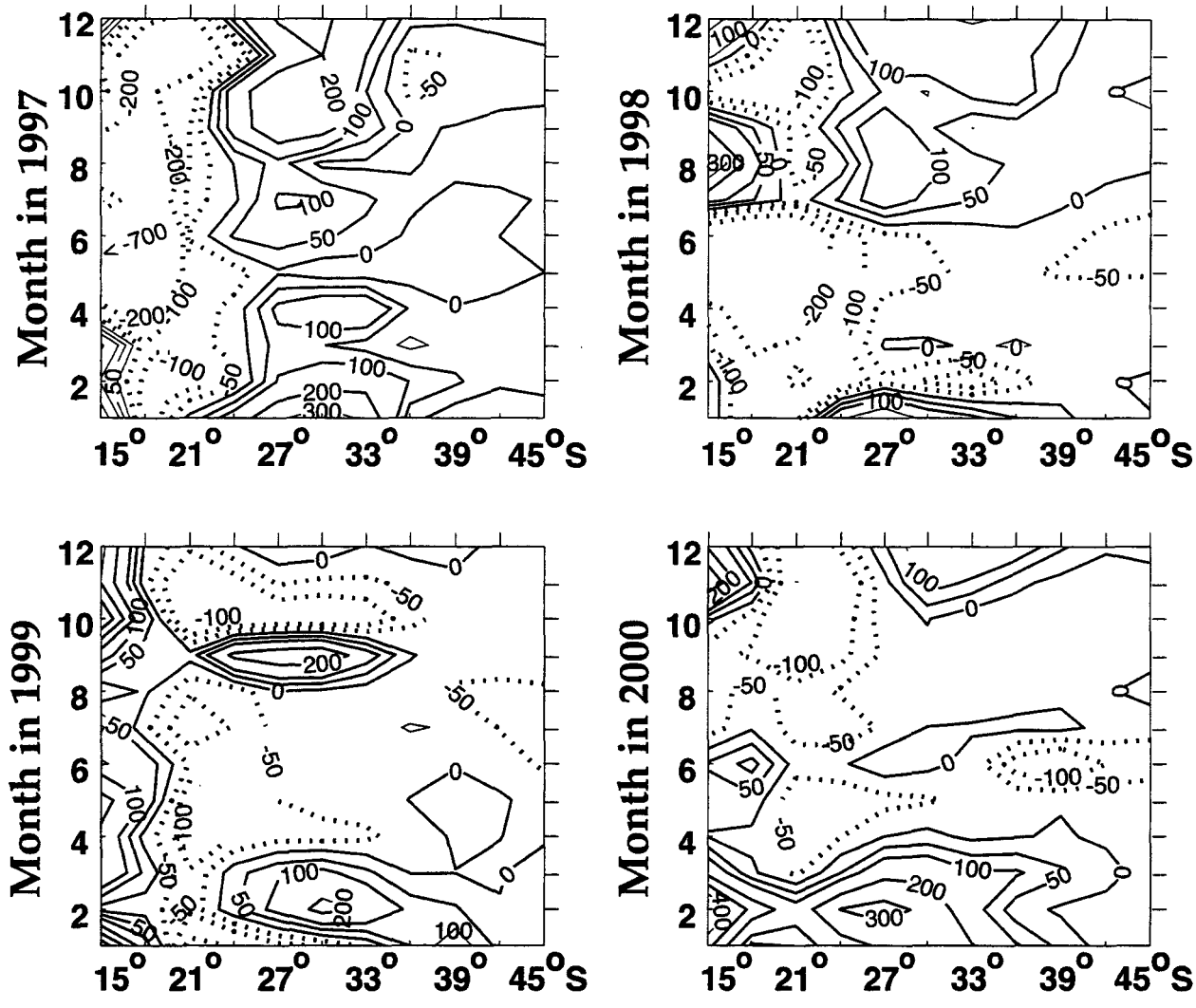

Figure 8 (continued). Contours are 0, 50, 100, 200 and 300 t/s/100m of coastline. Dotted contours show negative anomaly compared to the overall mean. Selected extreme values are indicated. Months are on the ordinate with January at the lower left. Abscissas show latitude from 15° to 45° S.

Time-space patterns of variability in UI anomaly may be latitudinal or seasonal. The latitudinal pattern shows uniformity of anomaly sign throughout the year (e.g., 1995). The seasonal pattern shows uniformity in anomaly sign across latitude (e.g. 1992). When both patterns occur together, as in 1996, the field is more complex. There is also the case where the anomaly has nearly the same sign and magnitude throughout the range of latitude for the entire year (e.g., 1985 or 1990, Figure 9).

In several years during the 20-year span, the Coastal and Offshore anomaly patterns have similar shape and magnitude in time-latitude space. However, there are usually some differences between the computation sets for a given latitude, and these differences may be partially due to the larger number across-land pressure interpolations that contribute to calculations at Coastal locations (COMPUTATIONS and ANALYSES). Inspection of the Coastal panels (Figure 8) shows shifting areas of extreme variability, which appear more intense in the austral fall and winter after about 1994. However, some sets of consecutive years have similar anomaly patterns (e.g., Coastal 1991, 1992, 1993). It is also seen that the smooth, apparently robust mean annual cycle shown in the first graph of the Figure 8 (and in Figure 4) is the result of averaging predominately anomalous patterns. The highest Coastal UI anomalies are found in the last half of the year at 30°S and northward. The

interannual variability at these locations will frequently exceed 500 t/s/100m coast (Appendix).

Initial El Niño - Southern Oscillation (ENSO) stages involve slackening of normally westward tropical trade winds across the eastern South Pacific (McCreary, 1976; Rasmusson and Wallace, 1983), which suggests weakening of the subtropical high atmospheric pressure system. Expected weakening of the high pressure system may be shown in negative UI anomaly found through the entire year at 15°S-18°S during the 1982, 1994, 1995 and 1997 periods of El Niño activity.

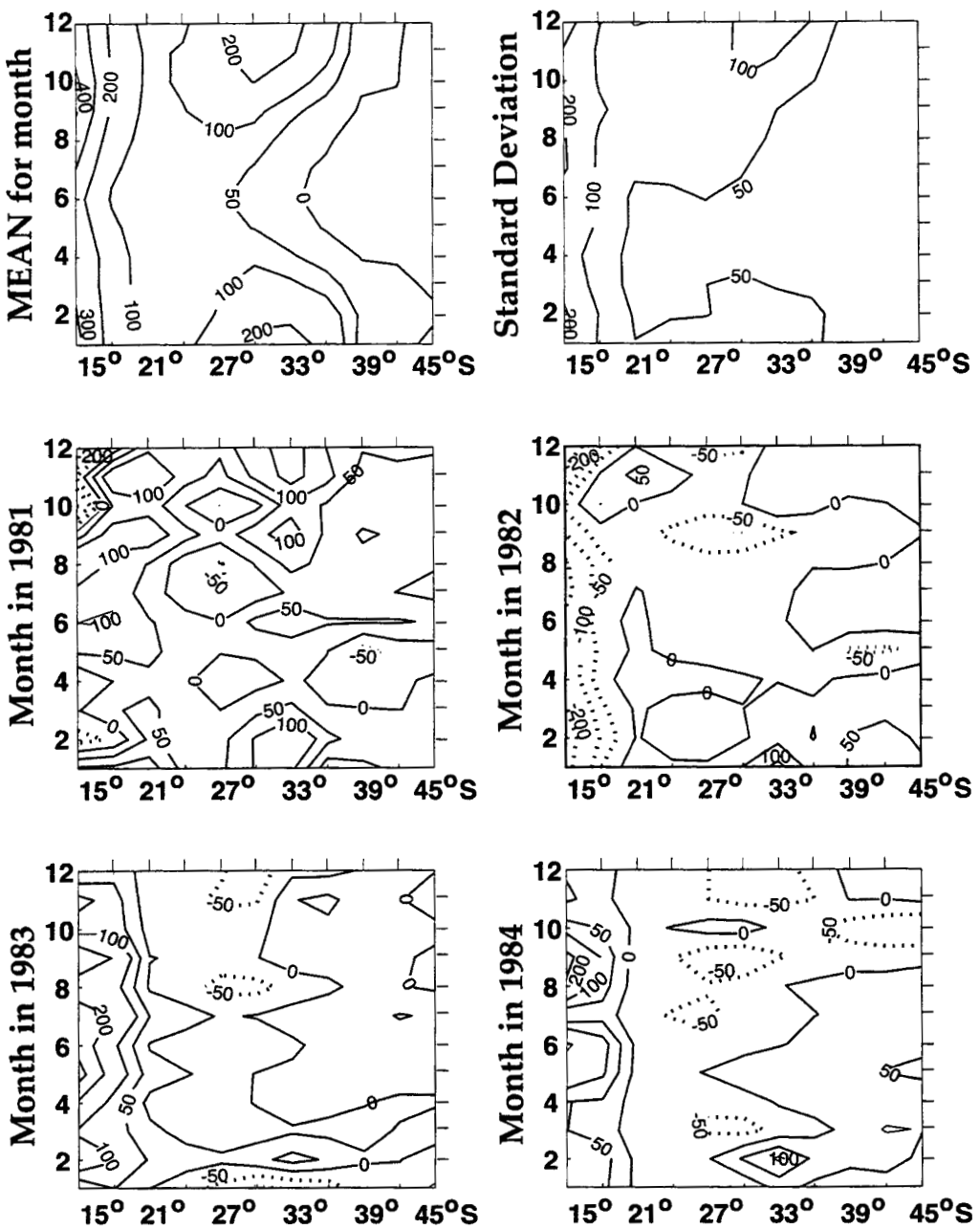

Figure 9. Mean annual cycles are contoured in the upper left panel for the Offshore locations. The overall standard deviation of monthly mean UI is upper right. The lower 20 panels show annual distribution of anomaly for the years 1981 to 2000. Contours are at 0, 50, 100, 200 and 300 t/s/100m of coastline. Dotted contours show negative anomaly compared to the overall mean. Selected extreme values are indicated. Months are on the ordinate with January at the lower left. Abscissas show latitude from 15° to 45° S.

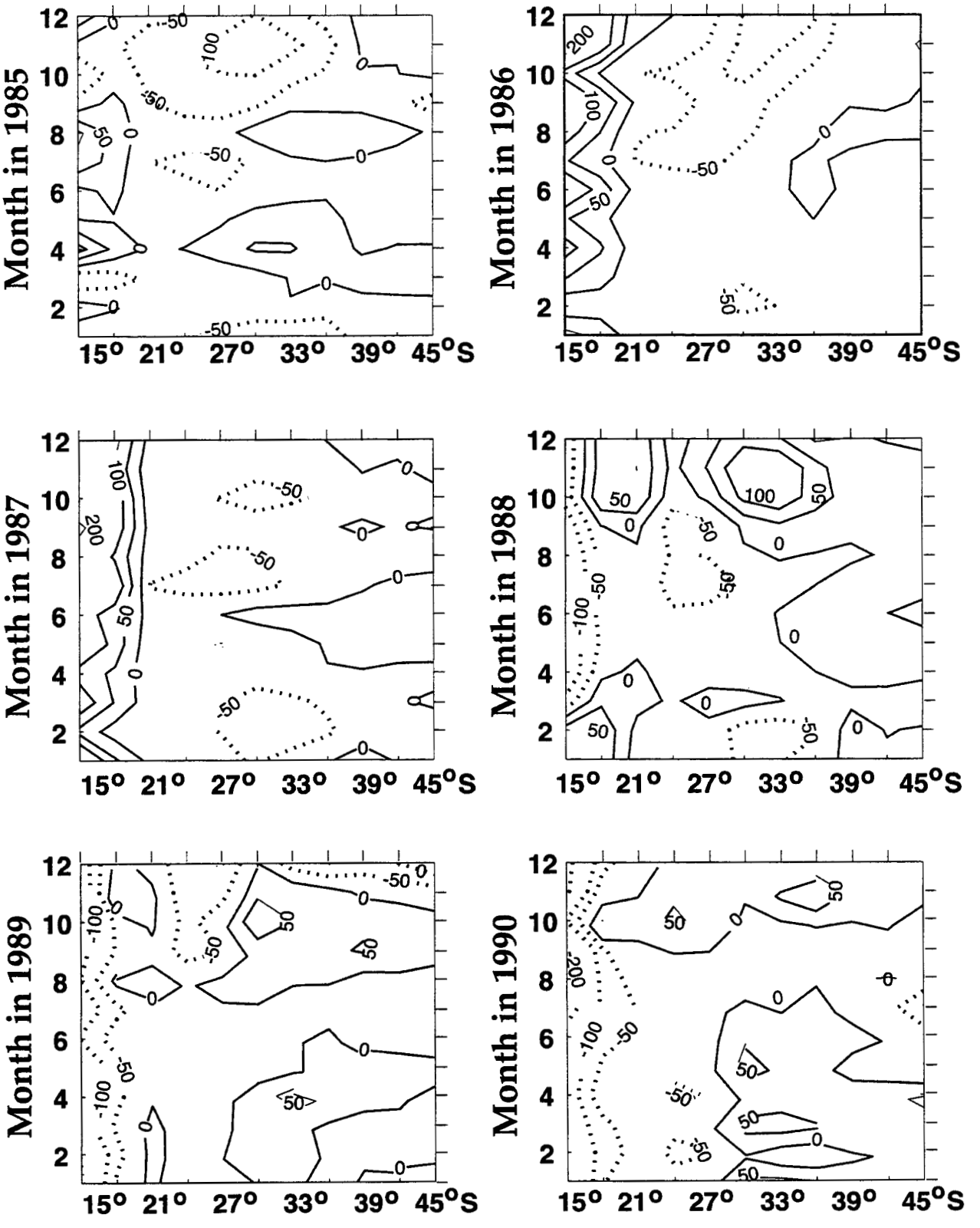

Figure 9 (continued). Contours are at 0, 50, 100, 200 and 300 t/s/100m of coastline. Dotted contours show negative anomaly compared to the overall mean. Selected extreme values are indicated. Months are on the ordinate with January at the lower left. Abscissas show latitude from 15° to 45° S.

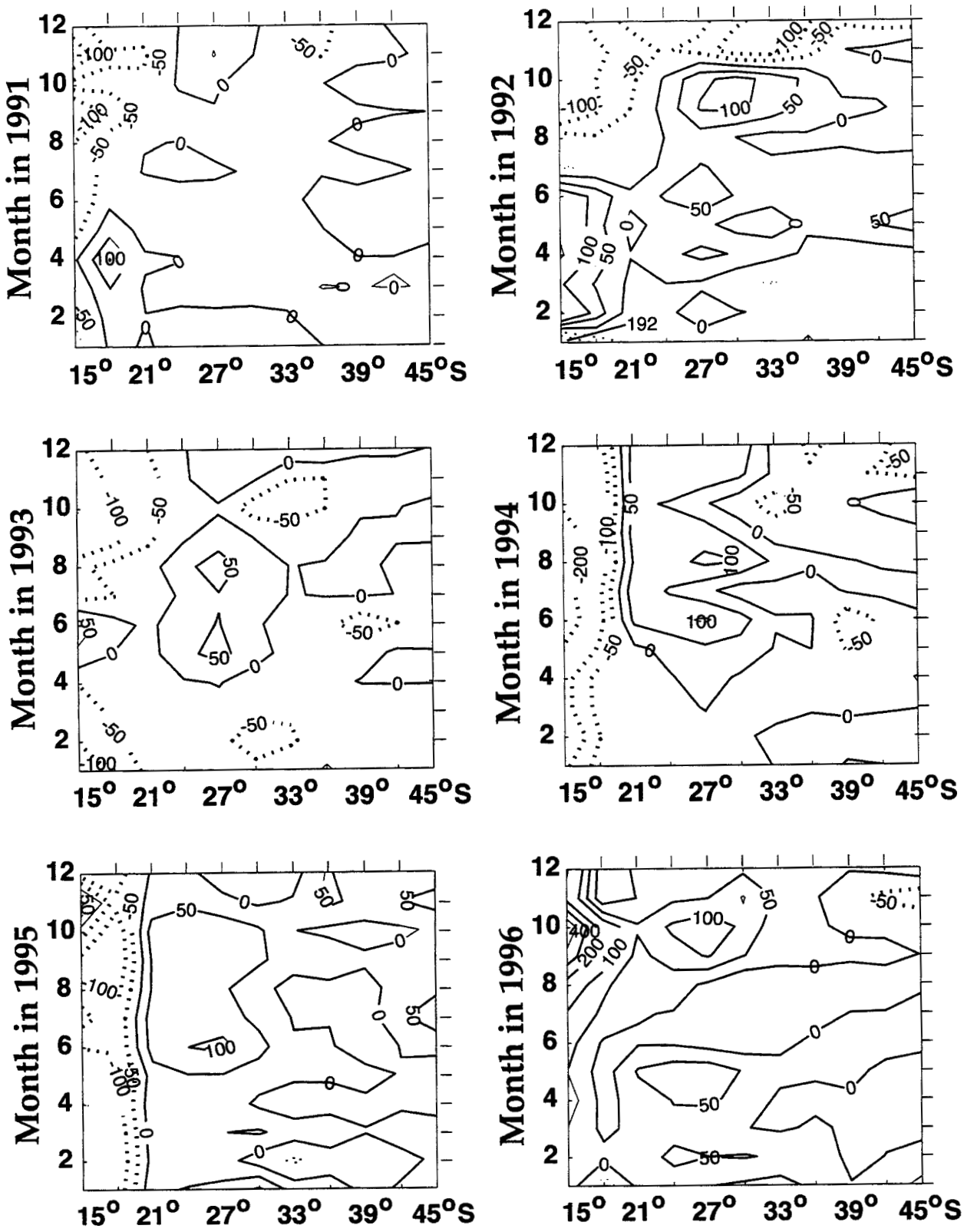

Figure 9 (continued). Contours are at 0, 50, 100, 200 and 300 t/s/100m of coastline. Dotted contours show negative anomaly compared to the overall mean. Selected extreme values are indicated. Months are on the ordinate with January at the lower left. Abscissas show latitude from 15° to 45° S.

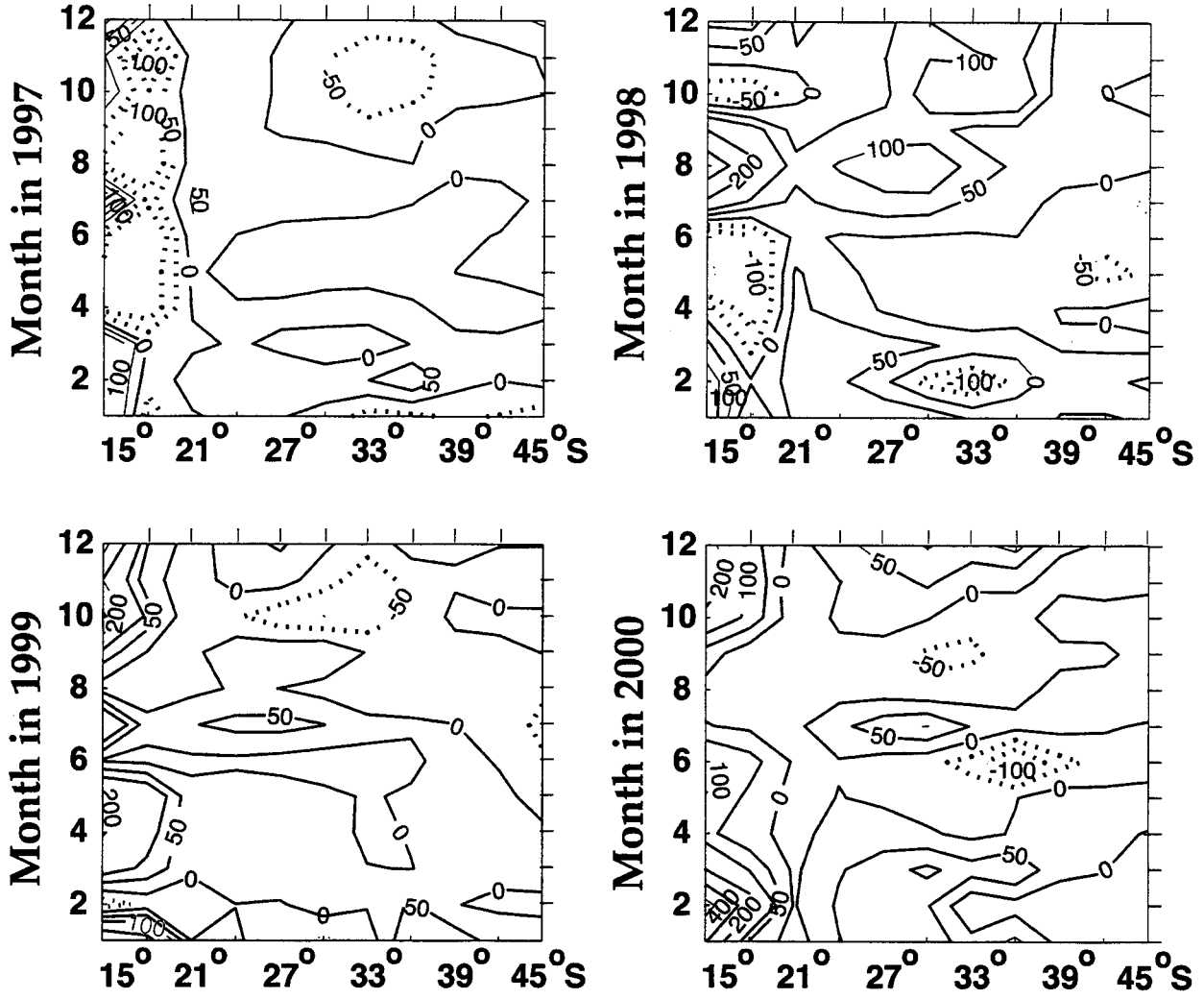

Figure 9 (continued). Contours are at 0, 50, 100, 200 and 300 t/s/100m of coastline. Dotted contours show negative anomaly compared to the overall mean. Selected extreme values are indicated. Months are on the ordinate with January at the lower left. Abscissas show latitude from 15° to 45° S.

DISCUSSION AND CONCLUSION

Off the coast of South America, highest UI values are in the austral spring and summer (October to March), with lower and frequently negative values in the austral winter (May to July). Overall averages and biharmonic analysis show that maximum UI occurs earlier in the year at the northern locations and appears to propagate to higher latitudes. The largest UI values are found north and south of the 21°S. North-to-south gradients in UI during the upwelling season appear related to distance from shore, adjacent land topography, and the intensity and persistence of the subtropical high atmospheric pressure system.

Interannual variation increases from south-to-north. North of 21°S, standard deviations may have three to four times the magnitude of the southern stations. Interannual variability may exceed the annual cycle in UI magnitude.

Several points are important in interpreting the UI. First, the FNMOC pressure field analysis is always the basis of these UI calculations. FNMOC analyses have become more sophisticated and intensive. Global FNMOC analyses have been refined to 1° x 1° grid length (see COMPUTATIONS and ANALYSES), but these analyses remain dependent on available observations which vary greatly depending on time period and region (Bakun and Nelson, 1991). Changes in

computation grid and observation density may be factors in retrospective studies involving the PFEL UI (e.g., Trenberth, 1995).

Herein, all UI calculations are from monthly mean pressure fields, and use a doubled drag coefficient, C_d = 0.0026. Doubling the value, relative to the six-hourly computation, compensates for smoothing of pressure gradients when the month's six-hourly pressure fields are averaged (Bakun, 1973; Schwing et al., 1996). Reduction of pressure gradients will reduce geostrophic wind speed proportionately (Equations 1 and 2).

Schwing et al. (1996), in their report on UI along the west coast of North America, present monthly climatologies in UI calculated from six-hourly pressure fields and the UI calculated from the monthly mean pressure, as described in this report. These comparisons show that, because of the non-linear linkage between geostrophic winds and the upwelling index computed from them (Bakun, 1973), the UI computed from the monthly mean field using the doubled drag coefficient will, in the mean, be equal or larger in magnitude than the monthly UI computed from six-hourly UI.

Mean magnitude of differences between the two methods decreases as the ratio of variance to directional consistency decreases. For months and locations where the variance to mean ratio is low (e.g., October to March at 36°N x 122°W), doubling the C_d provides reasonable agreement between methods. However, if computed UI is consistently negative, then the UI values computed from monthly mean fields will average less than the mean UI computed from six-hourly pressure fields. This is seen during January and February at 57°N x 137° W, 60°N x 146°W and 60°N x 149°W (Schwing et al., 1996, Appendix A). Although the calculations from monthly mean fields are consistently less (overestimate downwelling), they fall within one standard deviation of the mean of UI calculated from six-hourly pressure fields.

If UI is consistently positive as in spring and summer off central and southern California, UI calculated from the mean fields will be greater than (overestimate upwelling) those calculated from the six-hourly pressure fields. This is the case at 30°N x 119°W, 33°N x 119°W and 36°N x 122°W (Schwing et al., 1996, Appendix A). During May and June at these lower latitude locations UI calculated from monthly mean pressure fields may be more than one standard deviation greater than UI calculated from six-hourly pressure fields. (Schwing et al., 1996, Appendix). These caveats notwithstanding, Bakun (1973) found that UI derived by the two calculation methods had overall correlation coefficients greater than 0.93 at all North American locations from 21°N to 60°N, indicating relative consistency within and between each of the two time series at each computation location.

If needed, the user may recompute an Upwelling Index using source east and north geostrophic wind components (Thompson et al., 1983; Wright and Thompson, 1983) from files of Comprehensive Air/Ocean Flow Indices available at the PFEL Internet site:

ftp://www.pfeg.noaa.gov/outgoing/
So.Amer_arrowmark_indices/

The technique used to convert sea level atmospheric pressure analysis to offshore Ekman transport (UI) is based on a suite of simplifying assumptions that do not account for time-space variability in ocean surface roughness, sea surface layer stratification (Price and Sundermeyer, 1999), subsurface topography (Hickey, 1998; Strub et al., 1998), and remotely forced ocean processes (Smith, 1978, 1983; Rienecker and Mooers, 1986; Chelton and Schlax, 1996) that may contribute significantly to patterns of momentum transfer in particular areas.

FMNOC analyses and PFEL interpolations smooth sea level pressure gradients so that the UI produced is most appropriately used to represent processes of 100 to 500 km coastal extent, depending on the observational density available to FNMOC analyses. This smoothing may be valuable in fisheries studies that involve populations occupying areas exceeding 1000 km^2. The scaling similarities may enhance elucidation of innate relationships.

Another important aspect of the UI, making it useful in living marine resource studies, is its continuity. By using global forecasts as analysis initiators, FNMOC uses knowledge of previous conditions to reduce problems arising from sampling discontinuities (Rosemond, 1992). This leads to integration on synoptic time scales and provides continuously updated global sea level pressure analyses. Consequently, there are always UI values available to match the temporal span of sampling programs.

Finally, ocean upwelling frequently enhances nutrient supply to primary producers in the euphotic zone, the critical first step in producing new organic carbon compounds for coastal ecosystems. The PFEL UI is closely related to this vital first step and has been used effectively in hundreds of studies to explain differences in ocean productivity at various tropic levels (e.g. Parrish et al., 1981; Norton, 1987; Ainley et al., 1995; VenTresca *et al.*, 1995).

REFERENCES

Ainley, D. G., W. J. Sydeman and J. G. Norton, Upper trophic level predators indicate interannual negative and positive anomalies in the California Current food web, *Mar. Ecol. Prog. Ser., 118*, 69-79, 1995.

Bakun, A., Coastal upwelling indices, west coast of North America, 1946-71, 103 pp., NOAA Tech. Rep. NMFS SSRF-671, 1973.

Bakun, A., Daily and weekly upwelling indices, west coast of North America, 1967-73, 114 pp., NOAA Tech. Rep. NMFS SSRF-693, 1975.

Bakun, A. and G. S. Nelson, The seasonal cycle of wind-stress curl in subtropical eastern boundary current regions, *J. Phys. Oceanogr., 21*, 1815-1834, 1991.

Blanco, J. L., A. C. Thomas, M. E. Carr and P. T. Strub, Seasonal climatology and hydrographic conditions in the upwelling region off northern Chile, *J. Geophys. Res, 106,* 11451-11468, 2001.

Botsford, L. W. and D. E. Wickham, Correlation of upwelling index and Dungeness crab catch, *Fish. Bull. 73*, 901-907, 1975.

Cane, M. Oceanographic events during El Niño. *Science, 222*, 1189-1194, 1983.

Chavez, F. P., P. G. Strutton, G. E. Friederich, R. A. Feely, G. C. Feldman, D. G. Foley, M. J. McPhaden. Biological and chemical response of the equatorial Pacific Ocean to the 1997-98 El Niño, *Science, 286*, 2126-2131, 1999.

Chelton, D. B., M. G. Schlax. Global observations of oceanic Rossby waves, *Science, 272*, 234-238, 1996.

Clancy, R. M., Operational Modeling: Ocean Modeling at the Fleet Numberical Oceanography Center, *Oceanography, 5*, 31-35, 1992.

Cury, P., C. Roy, R. Mendelssohn, A. Bakun, D. M. Husby and R. H. Parrish, Moderate is better: exploring nonlinear clematic effects on the California northern anchovy (Engraulis mordax), *Can. Spec. Publ. Fish. Aquat. Sci., 121*, 415-424, 1995.

Davidson, K. L., Observational results on the influence of stability and wind-wave coupling on mementum transfer and turbulent fluctuations over ocean waves, *Boundary-Layer Met. 6*, 305-331, 1974.

Durand, M.-H, P. Cury, R. Mendelssohn, C. Roy, A. Bakun, D. Pauly, Eds. Global versus local changes in upwelling systems, 593 pp., Orstrom Editions. Paris 1998.

Ekman, V. W., On the influence of the earth's rotation on ocean currents, *Ark. Mat, Astron. Pys. 2*, 1-52, 1905.

Hickey, B. M. Coastal Oceanography of western North America from the tip of Baja California to Vancouver Island, 345-393, In *The Sea,* Volume 11, A. R. Robinson and K. H. Brink, Eds., 1998.

Hill, E. A., B. M. Hickey, F. A. Shillington, P. T. Strub, K. H. Brink, E. D. Barton; A. C. Thomas, Eastern Ocean Boundaries, 29-67, In *The Sea,* Volume 11, A. R. Robinson and K. H. Brink, Eds., 1998.

Huyer, A., Coastal upwelling in the California current system, *Progr. Oceanogr. 12*, 259-284, 1983.

Large, W., S. Pond. Open ocean momentum flux measurements in moderate to strong winds, *J. Phys. Oceanog.11* 324-336, 1981.

Lynn, R. J., Seasonal variation of temperature and salinity at 10 meters in the California Current, *Calif. Coop. Ocean. Fish. Invest. Rept. 11*, 157-173, 1967.

Maeda, S. and R. Kishimoto, Upwelling off the coast of Peru, *J. Oceanog. Soc. Japan 26,* 300-309, 1970.

Mann, K. H.; J. R. N. Lazier, Dynamics of Marine Ecosystems, Biological-Physical Interactions in the ocean, second edition, 394 pp., Blackwell Science, Inc, Cambridge, Massachusetts, 1996.

Mason, J. E. and A. Bakun, Upwelling index update U. S. west coast 33N - 48N latitude, 81 pp., NOAA Tech. Memo. NOAA-TM-NMFS-SWFC-67, 1986.

McCreary, J. Eastern tropical response to changing wind systems: with application to El Niño. *J. Phys. Oceanogr., 6*, 632-645, 1976.

Nelson, C. S., Wind stress and wind stress curl over the California current, 87 pp., NOAA Tech. Memo. NOAA-TM-NMFS SSRF 714, 1977.

Norton, J. G., Ocean climate influences on groundfish recruitment in the California current, 73-98, In Proceedings of the International Rockfish Symposium, October 20-22, 1986, Alaska Sea Grant College Program, University of Alaska, Fairbanks, Alaska., 1987.

Parrish, R., C. Nelson and A. Bakun, Transport mechanisms and reproductive success of fishes in the California current, *Biol. Oceanog. 1*, 175-203, 1981.

Peterson, W. T. and C. B. Miller, Seasonal cycle of zooplankton abundance and species composition along central Oregon coast, *Fish. Bull. 75,* 717-724, 1977.

Price, J. F., M. A. Sundermeyer, Stratified Ekman layers. *J. Geophys. Res. 104,* 20,467-20,494, 1999.

Rasmusson, E. M. and J. M. Wallace, Meteorological aspects of the El Niño/Southern Oscillation. *Science 122*, 1195-1202, 1983

Richards, F. A., Ed., Coastal Upwelling. 529 pp., American Geophysical Union, Washington, D. C., 1981.

Rosmond, T. E., A prototype fully coupled Ocean-Atmosphere Prediction System. *Oceanography 5*, 25-30, 1992.

Rienecker, M. M. and C. N. K. Mooers, The 1982-1983 El Niño signal off Northern California. *J. Geophys. Res., 91*, 6597-6608, 1986.

Ryther, J. H. Photosynthesis and fish production in the sea, *Science, 166*: 72-80, 1969.

Schwing, F. G., M. O'Farrell, J. Steger and K. Baltz, Coastal upwelling indices, west coast of North America 1946-1995., 207 pp., NOAA Tech. Rep., NOAA-TM-NMFS-SWFSC-231, 1996.

Smith, Robert L. Upwelling, *Oceanogr. Mar. Biol. Ann. Rev., 6*, 11-46, 1968.

Smith, R. L., D. B. Enfield, T. S. Hopkins and R.D.Pillsbury, The circulation in an upwelling ecosystem: the Pisco cruise, *Inv. Pesq. 35, 9-24*, 1971.

Smith, R. L., Poleward propagating perturbations in currents and sea levels along the Peru coast, *J. Geophys. Res. 83*, 6083-6092, 1978.

Smith, R. L., Peru coastal currents during El Niño: 1976 and 1982, *Science 222*, 1397-1398, 1983.

Strub, P. Ted, J. M. Mesias, Vivian Montecino, Jose' Rutllant, Coastal ocean circulation of western South America, 273-313, In The Sea, Volume 11, A. R. Robinson and K. H. Brink, Eds., John Wiley and Sons, Inc., 1998.

Sverdrup, H. U., M. W. Johnson and R. H. Fleming, The Oceans, their physics, chemistry and general biology, 1087 pp., Prentice-Hall, New Jersey, 1942.

Thomas, A. C., F. Huang, P. T. Strub and C. James, Comparison of the seasonal and interannual variability of phystoplankton pigment concentrations in the Peru and California Current systems, *J. Geophys. Res. 99*, 7355-7370, 1994.

Thompson, K. R., R. F. Marsden and D. G. Wright, Estimation of low-frequency wind stress fluctuations of the open ocean, *J. Phys. Oceanog., 13*, 1003-1011, 1983.

Traganza, E., J. C. Conrad and L. C. Breaker, Satellite observations of a cyclonic upwelling system and giant plume in the California Current, 228-241, In Coastal Upwelling, American Geophysical Union, F. A. Richards, Ed, 1981.

Trenberth, K. E. Atmospheric circulation climate changes, *Climate Change, 31* , 427-453, 1995.

Trenberth, K. E.; W. G. Large, J. G. Olson. The mean annual cycle in global wind stress, *J. Phys. Oceanog., 20*, 1742-1760, 1990.

VenTresca, D. A., R. H. Parrish, J. L. Houk, M. L. Gingras, S. D. Short and N. L. Crane, El Niño effects on the somatic reproductive condition of blue rockfish, Sebastes mystinus, *Calif. Coop. Oceanic Fish Invest. Rep. 36*, 167-174, 1995.

Wooster, W. S., J. L. Reid, Jr. Eastern Boundary Currents, 253-280, In M.N. Hill, Ed., The Sea, Volume 2, Interscience, New York, 1963.

Wright, D. G. and K. R. Thompson, Time-averaged forms of the nonlinear stress law, *J. Phys. Oceanog., 13*, 341-345, 1983.

APPENDIX

Coastal Upwelling Index (t/s/100m shore)

year	mo	15x76	18x72	21x71	24x71	27x72	30x72	33x72	36x73	39x74	42x75	45x75
1981	1	389	299	360	289	238	266	271	160	34	31	27
1981	2	202	119	160	140	137	170	223	209	82	62	31
1981	3	282	214	200	138	112	121	125	82	21	17	5
1981	4	197	109	85	67	47	43	43	16	-2	-7	-13
1981	5	300	186	209	172	116	73	27	1	-85	-62	-61
1981	6	291	157	77	50	31	45	54	32	3	20	4
1981	7	303	169	69	46	21	17	9	3	-17	-21	-50
1981	8	484	221	166	105	50	49	69	38	2	-2	-17
1981	9	362	207	126	114	90	102	131	68	6	9	2
1981	10	209	213	234	251	171	164	171	112	36	27	7
1981	11	299	268	345	399	298	314	358	258	74	51	5
1981	12	121	117	222	287	274	324	371	262	84	74	48
1982	1	87.5	89	179	226.5	207	231	269.5	201.5	81	81.5	48.5
1982	2	54	61	136	166	140	138	168	141	78	89	49
1982	3	77	65	88	100	88	88	100	83	40	52	31
1982	4	104	69	58	63	80	58	42	22	3	7	9
1982	5	97	55	67	73	65	35	12	-1	-60	-80	-77
1982	6	72	62	72	87	50	21	5	-2	-13	-1	-8
1982	7	54	45	61	79	55	20	4	0	-14	-9	-10
1982	8	119	52	92	107	88	61	33	6	-18	-18	-18
1982	9	299	132	143	135	82	44	12	-1	-23	-26	-19
1982	10	389	267	262	283	228	231	211	115	21	17	5
1982	11	178	140	221	280	236	254	237	143	56	55	24
1982	12	57	79	159	199	169	204	235	195	79	47	9
1983	1	292	184	291	283	209	215	165	109	37	22	7
1983	2	384	129	199	171	148	207	217	198	77	42	12
1983	3	324	124	160	133	109	144	130	82	22	19	13
1983	4	457	140	147	110	80	96	83	49	7	0	-16
1983	5	544	146	149	109	67	57	33	8	-7	-16	-26
1983	6	443	76	41	41	19	9	1	0	-12	-6	-12
1983	7	498	175	127	101	65	42	22	15	-2	23	0
1983	8	466	182	144	107	49	23	4	-1	-10	-14	-32
1983	9	753	318	238	208	159	147	103	58	13	10	-16
1983	10	506	269	405	411	330	324	216	129	45	34	14
1983	11	495	237	308	299	252	288	250	201	75	35	-12
1983	12	371	247	394	413	318	325	270	168	54	32	10
1984	1	403	222	390	410	311	329	277	194	51	18	-19
1984	2	322	168	281	326	282	331	303	206	66	53	17
1984	3	346	175	157	134	90	87	73	60	29	9	0
1984	4	344	96	53	47	36	38	44	47	17	17	-1
1984	5	448	170	298	322	201	155	77	19	-10	13	12
1984	6	439	111	63	50	21	11	6	0	-11	-6	-7
1984	7	312	99	159	141	59	21	1	-6	-26	-24	-29
1984	8	553	190	88	50	41	35	26	16	2	3	-6
1984	9	703	356	333	235	111	67	25	1	-16	-23	-26
1984	10	557	341	491	526	411	380	195	44	-18	-52	-86
1984	11	429	241	324	365	304	301	179	84	22	13	2
1984	12	379	179	241	247	217	235	169	114	39	26	18

year	mo	15x76	18x72	21x71	24x71	27x72	30x72	33x72	36x73	39x74	42x75	45x75
1985	1	338	128	248	298	235	233	157	100	28	10	-13
1985	2	292	89	173	183	161	182	157	123	39	25	9
1985	3	199	81	173	198	156	169	128	85	35	35	33
1985	4	414	123	141	162	142	150	116	51	5	5	-15
1985	5	266	51	99	134	114	111	59	13	-25	-25	-44
1985	6	199	16	54	66	17	2	-2	-17	-45	-38	-28
1985	7	392	75	75	76	33	8	0	-3	-17	-27	-36
1985	8	475	119	91	89	73	75	56	36	7	4	-25
1985	9	411	168	182	166	95	73	46	18	-2	-20	-62
1985	10	389	334	325	326	218	194	105	37	8	4	-1
1985	11	475	339	261	298	226	214	121	56	21	14	1
1985	12	561	394	335	363	273	270	193	134	54	22	15
1986	1	451	252	329	430	385	388	238	145	44	13	-16
1986	2	309	176	200	227	177	183	136	99	37	14	-8
1986	3	376.5	183.5	190	216.5	155.5	143.5	92	54	12.5	-1.5	-16.5
1986	4	444	191	180	206	134	104	48	9	-12	-17	-25
1986	5	354	128	164	188	114	77	26	1	-43	-44	-48
1986	6	399	133	118	126	65	37	10	-1	-40	-35	-52
1986	7	340	56	18	14	10	9	5	0	-15	-38	-62
1986	8	532	177	145	128	58	29	7	0	-7	-7	-20
1986	9	579	181	144	153	112	76	28	6	-2	-8	-12
1986	10	549	203	203	244	193	141	71	39	9	0	-9
1986	11	698	384	488	563	416	352	169	57	12	8	-11
1986	12	698	384	488	563	416	352	169	57	12	8	-11
1987	1	486	175	273	301	257	268	202	174	78	28	3
1987	2	285	71	73	114	127	125	84	83	44	13	-5
1987	3	451	163	132	149	123	101	48	32	14	8	6
1987	4	380	143	75	70	58	62	43	23	2	-9	-30
1987	5	464	209	26	8	6	6	2	1	0	-1	-7
1987	6	350	109	39	35	42	44	24	10	-7	-17	-25
1987	7	553	377	269	238	81	20	-4	-38	-55	-20	-14
1987	8	549	212	130	110	61	25	1	-3	-19	-35	-63
1987	9	706	379	235	212	157	110	49	24	3	-2	-8
1987	10	694	578	395	374	292	224	91	36	6	0	-11
1987	11	625	440	367	361	314	302	174	111	36	12	3
1987	12	587	411	323	322	287	277	187	154	60	29	12
1988	1	455	305	358	421	319	287	185	140	69	35	23
1988	2	405	284	82	78	93	83	70	76	60	34	25
1988	3	201	211	229	225	193	162	111	66	17	9	-20
1988	4	174	139	107	68	53	41	27	21	10	12	0
1988	5	132	54	3	-1	2	8	5	3	1	2	-4
1988	6	120	60	34	15	11	15	8	5	-15	-16	-51
1988	7	136	45	2	3	0	-4	-12	-12	-9	-6	-8
1988	8	245	146	147	109	81	82	46	6	-19	-14	-4
1988	9	332	257	222	130	91	102	82	48	13	9	1
1988	10	439	411	459	329	289	308	258	153	50	42	26
1988	11	360	357	489	422	416	423	352	221	61	31	10
1988	12	383	402	568	485	455	459	327	177	49	34	18
1989	1	157	188	283	256	258	264	226	163	65	49	32
1989	2	112	111	197	207	218	243	197	136	57	33	21

year	mo	15x76	18x72	21x71	24x71	27x72	30x72	33x72	36x73	39x74	42x75	45x75
1989	3	167	126	167	150	143	145	116	71	19	14	6
1989	4	133	63	77	81	79	87	91	68	19	19	-6
1989	5	87	17	6	9	13	14	10	4	0	-3	-15
1989	6	145	50	55	48	37	30	15	2	-42	-42	-60
1989	7	136	20	23	32	30	13	0	-15	-54	-42	-54
1989	8	251	167	202	187	167	176	99	19	-39	-31	-53
1989	9	307	149	138	92	102	126	74	47	51	45	25
1989	10	269	207	279	237	266	344	227	100	65	60	37
1989	11	273	402	482	333	330	467	376	200	87	49	28
1989	12	327	479	545	322	329	580	443	116	13	-10	-73
1990	1	127	143	275	292	333	500	452	296	162	94	71
1990	2	138	128	138	67	106	208	179	108	81	78	56
1990	3	134	84	122	113	126	195	181	131	82	69	50
1990	4	165	177	141	81	76	129	109	53	29	39	46
1990	5	113	62	29	12	31	92	80	15	-19	-35	-71
1990	6	59	-4	-20	-11	1	25	29	12	-11	-11	-35
1990	7	29	0	-5	0	24	39	14	1	-19	-25	-74
1990	8	79	47	93	125	158	140	70	14	-7	1	-13
1990	9	182	132	89	74	108	112	46	5	-17	-15	-30
1990	10	443	389	425	473	499	533	359	129	52	62	38
1990	11	210	220	403	472	532	664	544	307	165	142	86
1990	12	173	165	278	363	475	602	476	235	102	93	66
1991	1	244	267	271	291	417	581	475	247	97	66	24
1991	2	257	247	230	229.5	301.5	424.5	347.5	176.5	79.5	62.5	44
1991	3	270	227	189	168	186	268	220	106	62	59	64
1991	4	293	225	158	159	170	168	97	22	8	18	-1
1991	5	208	149	100	100	94	84	40	3	-13	9	23
1991	6	121	61	22	19	26	16	2	-4	-18	-4	0
1991	7	166	47	81	93	115	76	20	-3	-41	-23	-19
1991	8	215	79	98	85	89	64	21	1	-3	-1	-2
1991	9	194	73	132	152	198	180	98	19	-6	3	-2
1991	10	337	142	204	207	234	201	110	65	45	46	33
1991	11	197	136	213	252	342	395	290	115	27	21	9
1991	12	272	203	385	410	426	519	415	151	35	46	19
1992	1	114	53	183	259	289	375	358	233	97	61	16
1992	2	441	157	72	120	175	225	216	153	67	45	33
1992	3	298	100	117	130	147	163	139	62	17	9	0
1992	4	407	133	146	162	193	187	128	35	-11	-16	-30
1992	5	374	129	187	191	169	100	33	5	-3	21	20
1992	6	272	86	214	257	246	156	49	3	-29	-15	-17
1992	7	137	4	4	9	55	51	12	0	-4	-4	-12
1992	8	254	48	51	65	99	69	18	0	-19	-42	-63
1992	9	164	51	57	61	143	152	100	58	21	19	-18
1992	10	234	82	174	203	297	379	311	161	39	38	-6
1992	11	214	68	166	170	176	171	105	51	28	29	19
1992	12	166	109	252	256	272	356	309	103	5	-25	-67
1993	1	114	53	183	259	289	375	358	233	97	61	16
1993	2	165	44	52	65	82	98	121	136	73	20	-2
1993	3	146	41	103	114	111	126	123	54	10	9	-12
1993	4	192	32	103	119	111	95	51	18	5	8	-9

year	mo	15x76	18x72	21x71	24x71	27x72	30x72	33x72	36x73	39x74	42x75	45x75
1993	5	238	72	213	254	243	182	50	-5	-65	-27	-37
1993	6	201	26	179	190	152	82	9	-29	-114	-83	-80
1993	7	150	9	72	71	86	63	8	-4	-29	-24	-47
1993	8	221	41	139	172	194	113	32	9	1	-7	-32
1993	9	205	28	158	178	173	136	61	20	6	9	3
1993	10	212	70	225	246	237	197	95	28	7	6	2
1993	11	246	122	345	433	457	503	349	129	30	23	-4
1993	12	266	129	327	390	408	476	424	260	114	72	35
1994	1	224	129	272	293	292	375	354	239	120	71	36
1994	2	103	44	122	135	140	205	239	195	132	118	104
1994	3	135	48	87	110	127	127	112	80	33	23	8
1994	4	132	36	69	101	127	108	59	16	-1	-1	-7
1994	5	-23	-34	119	207	236	202	85	3	-53	-56	-61
1994	6	-475	-478	96	241	339	259	104	8	-85	-48	-42
1994	7	-271	-380	76	249	272	76	2	-21	-44	-11	-9
1994	8	-126	-286	82	213	364	264	140	39	1	6	-27
1994	9	54	-80	580	766	641	353	129	13	-18	-6	-12
1994	10	176	-49	276	444	561	492	232	65	25	55	59
1994	11	95	-105	267	554	784	805	568	180	15	7	-39
1994	12	121	-24	404	791	1021	1127	728	232	33	16	-26
1995	1	79	-72	230	392	563	699	507	281	105	75	46
1995	2	55	-86	102	177	323	349	254	155	79	61	43
1995	3	15	-167	85	186	349	409	285	154	80	84	52
1995	4	120	-164	43	190	334	233	105	14	-2	14	-18
1995	5	-67	-361	-3	42	156	90	38	10	-2	-5	-37
1995	6	-84	-277	242	446	442	279	95	6	-73	-17	-27
1995	7	114	-159	193	468	450	312	128	9	-62	22	28
1995	8	161	-131	28	236	461	326	106	5	-31	3	-5
1995	9	190	-50	289	459	550	331	158	90	37	54	26
1995	10	313	-21	297	524	724	645	384	129	29	38	22
1995	11	501	13	352	626	760	724	545	289	141	131	109
1995	12	233	-20	189	360	524	647	554	322	153	86	57
1996	1	377	1	262	422	521	637	530	296	137	128	107
1996	2	335	40	108	259	391	462	403	239	110	100	71
1996	3	343	22	13	71	219	273	218	115	56	55	24
1996	4	358	-5	59	201	288	205	107	27	3	-2	-38
1996	5	222	-72	-7	41	200	146	72	11	-5	-9	-40
1996	6	186	-170	-166	-1	25	3	-10	-10	-13	-9	-7
1996	7	278	-17	-45	6	60	4	-14	-30	-41	-26	-25
1996	8	469	54	148	333	341	187	54	-2	-47	-37	-41
1996	9	775	136	124	256	356	192	95	50	19	36	17
1996	10	1021	137	101	458	790	709	436	149	38	36	14
1996	11	510	21	65	275	611	865	696	255	35	2	-41
1996	12	592	11	150	480	748	846	684	255	80	55	50
1997	1	617	0	270	481	646	774	631	236	50	26	-20
1997	2	371	-38	8	101	325	414	393	257	138	58	59
1997	3	486	8	42	112	246	244	178	76	58	40	18
1997	4	85	-256	-16	64	245	290	251	73	8	8	5
1997	5	-123	-755	-36	18	95	43	2	-26	-57	-28	-35
1997	6	-387	-1196	-8	151	176	121	56	-19	-69	-32	-26

year	mo	15x76	18x72	21x71	24x71	27x72	30x72	33x72	36x73	39x74	42x75	45x75
1997	7	161	-354	-21	82	206	166	81	7	-40	-30	-32
1997	8	-234	-766	-2	132	232	97	37	7	-2	2	-2
1997	9	231	-161	84	369	536	433	175	25	7	37	31
1997	10	361	-16	96	481	664	624	267	27	-14	-12	-18
1997	11	292	-147	2	175	538	668	449	106	10	7	-6
1997	12	554	23	54	471	655	724	564	226	80	62	55
1998	1	390	-2	137	525	665	585	469	268	98	32	21
1998	2	330	-31	-88	5	156	153	88	85	65	49	40
1998	3	222	-133	-66	23	181	200	143	94	27	14	-8
1998	4	116	-255	-268	-14	91	88	35	5	-1	-1	-9
1998	5	-313	-603	-271	-39	28	16	-3	-40	-86	-80	-92
1998	6	-249	-577	-412	-44	28	17	-5	-20	-81	-94	-106
1998	7	347	68	25	152	248	141	71	29	-16	-43	-75
1998	8	703	187	4	102	312	238	121	52	8	11	-16
1998	9	577	183	114	297	400	239	88	51	22	20	12
1998	10	290	25	98	313	426	400	339	238	65	25	-10
1998	11	470	119	79	361	576	632	507	288	116	54	30
1998	12	651	278	152	483	629	703	612	398	167	56	32
1999	1	811	285	23	146	248	327	309	267	229	85	51
1999	2	258	78	46	216	341	495	415	242	135	53	33
1999	3	459	126	18	172	268	311	213	86	38	29	18
1999	4	441	31	-76	0	55	42	15	11	10	5	-11
1999	5	436	85	-91	0	52	55	15	2	-1	-16	-57
1999	6	165	2	-20	8	51	30	1	-23	-52	-58	-98
1999	7	325	-24	-96	-2	66	46	10	-1	-30	-75	-118
1999	8	248	50	0	46	158	99	15	-8	-74	-79	-85
1999	9	528	137	202	457	512	467	229	35	-19	-14	-24
1999	10	953	301	55	149	204	180	65	24	7	3	-5
1999	11	700	149	66	223	373	405	291	128	44	16	-22
1999	12	720	182	204	388	485	550	401	228	88	24	7
2000	1	673	179	307	495	581	676	556	323	125	29	5
2000	2	836	376	268	476	560	535	359	181	70	40	15
2000	3	436	100	52	191	343	364	257	197	98	42	-2
2000	4	258	39	2	47	126	134	66	28	9	-1	-22
2000	5	216	19	-30	0	34	22	1	-9	-31	-34	-42
2000	6	180	35	9	85	131	79	5	-141	-231	-132	-124
2000	7	134	5	-18	1	61	60	25	8	-12	-36	-68
2000	8	200	25	11	87	130	74	11	-9	-29	-20	-7
2000	9	312	23	30	114	202	167	43	0	-23	-33	-24
2000	10	455	122	77	199	347	354	178	58	14	16	8
2000	11	803	280	63	183	398	599	437	181	36	9	-13
2000	12	577	175	133	307	486	669	591	359	130	46	33

Offshore Upwelling Index (t/s/100m shore)

year	mo	15x77	18x74	21X74	24X74	27x74	30x74	33x74	36x74	39x77	42x77	45x77
1981	1	441	275	194	110	184	338	349	143	20	25	14
1981	2	232	120	113	91	140	277	356	209	61	52	8
1981	3	288	193	122	69	91	166	179	79	16	12	-6
1981	4	245	146	88	67	54	69	63	14	-9	-11	-20
1981	5	320	178	121	69	65	56	30	-2	-110	-59	-64
1981	6	336	199	109	72	57	100	103	38	11	27	6
1981	7	363	202	82	49	20	17	17	5	-22	-26	-60
1981	8	550	223	114	43	38	77	100	38	-5	-10	-31
1981	9	438	318	211	169	148	200	192	65	-12	3	0
1981	10	228	254	165	111	120	184	217	116	36	29	2
1981	11	343	342	256	180	216	368	459	247	41	36	-15
1981	12	134	151	155	137	219	403	489	255	67	74	42
1982	1	95.5	110	106.5	88	150.5	283.5	352	198	79	86	45.5
1982	2	57	69	58	39	82	164	215	141	91	98	49
1982	3	85	87	64	42	71	129	140	81	40	48	25
1982	4	149	126	90	82	95	92	54	18	3	8	11
1982	5	113	84	61	43	46	29	7	-3	-89	-86	-80
1982	6	73	87	57	46	30	13	3	-2	-1	7	-6
1982	7	56	70	64	61	43	17	4	-1	-10	-7	-11
1982	8	142	82	49	55	63	55	30	5	-28	-21	-20
1982	9	310	162	47	37	34	15	1	-4	-37	-35	-25
1982	10	388	253	81	93	150	201	188	89	-5	0	-7
1982	11	221	199	152	128	168	249	237	131	43	52	21
1982	12	64	81	66	49	85	184	260	181	42	31	-19
1983	1	331	212	67	52	79	118	140	97	15	8	-10
1983	2	463	265	99	84	117	206	252	186	40	31	-6
1983	3	379	223	68	43	61	105	108	63	9	14	6
1983	4	484	219	41	37	57	92	85	40	-1	-9	-29
1983	5	604	262	78	57	49	50	27	4	-12	-17	-33
1983	6	499	202	48	30	11	4	0	-1	-6	0	-9
1983	7	575	304	110	93	70	48	30	17	4	28	-1
1983	8	481	274	58	46	25	7	0	-2	-9	-18	-45
1983	9	707	379	77	90	103	115	92	48	6	2	-31
1983	10	486	286	64	88	145	184	176	109	15	16	-6
1983	11	501	264	53	67	126	201	260	191	30	8	-60
1983	12	363	214	43	58	114	168	215	139	18	11	-19
1984	1	420	223	52	61	123	196	255	163	15	1	-49
1984	2	368	232	38	38	104	228	292	182	44	47	0
1984	3	342	180	19	15	35	63	79	62	29	10	-6
1984	4	352	190	27	26	37	62	65	45	10	10	-15
1984	5	422	228	29	37	68	89	64	14	-1	24	22
1984	6	450	217	34	23	13	9	3	0	-4	-1	-3
1984	7	300	141	20	21	18	8	-1	-8	-18	-17	-30
1984	8	542	221	36	40	46	43	29	14	4	6	-2
1984	9	638	278	45	51	46	26	8	0	-34	-36	-43
1984	10	493	250	72	111	191	225	125	26	-67	-85	-120
1984	11	374	208	41	68	133	186	151	77	15	7	-15
1984	12	367	199	41	51	110	175	171	113	36	28	14

year	mo	15x77	18x74	21X74	24X74	27x74	30x74	33x74	36x74	39x77	42x77	45x77
1985	1	302	124	21	33	82	134	140	86	11	2	-33
1985	2	326	165	33	34	91	167	181	119	22	17	-10
1985	3	199	72	18	23	59	106	118	81	33	32	25
1985	4	420	184	49	62	104	145	114	42	-7	-3	-23
1985	5	266	115	21	32	55	71	39	9	-47	-40	-61
1985	6	222	105	15	13	5	0	-7	-23	-52	-44	-47
1985	7	382	143	12	15	10	1	-1	-7	-34	-45	-53
1985	8	466	185	33	47	72	95	79	36	3	-3	-44
1985	9	375	207	28	31	45	55	44	15	-17	-41	-94
1985	10	321	170	27	30	72	100	69	28	3	0	-7
1985	11	366	149	10	19	68	110	98	55	17	7	-16
1985	12	446	193	29	44	95	144	163	125	25	11	-4
1986	1	401	193	39	61	141	214	209	136	18	0	-41
1986	2	265	134	18	26	62	111	134	97	19	5	-30
1986	3	344.5	168.5	24	31	58	83.5	82.5	51.5	-1	-6.5	-29
1986	4	424	203	30	36	54	56	31	6	-21	-18	-28
1986	5	321	133	15	27	39	33	11	-3	-68	-57	-62
1986	6	406	172	37	38	31	15	2	-4	-52	-39	-60
1986	7	353	125	10	10	9	11	5	0	-39	-60	-84
1986	8	488	200	17	25	22	11	2	0	-6	-5	-21
1986	9	612	288	67	71	68	49	21	5	-8	-12	-18
1986	10	498	200	37	51	84	86	65	35	-1	-9	-23
1986	11	652	330	87	89	134	147	104	47	-2	-4	-29
1986	12	652	330	87	89	134	147	104	47	-2	-4	-29
1987	1	516	218	51	56	108	175	213	172	41	14	-27
1987	2	337	136	24	28	55	79	90	84	22	7	-21
1987	3	432	194	23	24	45	59	54	37	12	7	2
1987	4	377	186	22	22	41	59	48	22	-7	-19	-44
1987	5	433	199	14	11	11	9	3	1	3	1	-8
1987	6	364	165	31	43	55	55	27	8	-22	-26	-39
1987	7	461	258	9	6	4	-20	-35	-51	-35	-13	-10
1987	8	522	241	38	41	34	16	2	-3	-31	-50	-84
1987	9	623	326	55	68	93	92	55	25	-1	-8	-16
1987	10	561	342	53	64	120	132	78	33	-6	-13	-31
1987	11	547	282	49	74	162	220	184	112	13	0	-19
1987	12	530	300	47	67	134	195	213	157	30	16	-13
1988	1	423	250	37	57	117	172	181	144	46	26	9
1988	2	379	252	37	50	88	99	103	88	62	27	13
1988	3	206	189	74	51	117	149	117	58	4	-3	-49
1988	4	142	131	69	29	47	54	39	24	11	12	-7
1988	5	123	76	36	24	27	33	18	6	4	2	-8
1988	6	101	57	21	6	15	23	10	4	-23	-26	-67
1988	7	123	67	26	16	6	1	-4	-8	-2	-4	-10
1988	8	185	113	58	21	44	67	34	5	-33	-13	-2
1988	9	270	186	87	26	64	127	103	49	12	6	-10
1988	10	342	294	182	75	183	317	282	147	31	26	-2
1988	11	295	262	187	92	237	404	373	198	21	8	-28
1988	12	273	256	163	59	191	328	284	148	14	6	-23
1989	1	119	122	78	27	118	231	244	155	36	29	5
1989	2	104	94	69	36	106	209	214	133	31	18	-3

year	mo	15x77	18x74	21X74	24X74	27x74	30x74	33x74	36x74	39x77	42x77	45x77
1989	3	157	110	69	34	83	152	131	63	3	0	-19
1989	4	132	84	55	36	66	120	124	64	5	0	-42
1989	5	91	46	33	40	37	29	16	3	-3	-8	-25
1989	6	144	68	39	30	39	28	3	-4	-66	-53	-79
1989	7	154	50	43	57	60	21	0	-21	-65	-54	-81
1989	8	257	162	100	69	113	118	31	6	-69	-44	-75
1989	9	296	140	60	24	78	138	95	61	54	27	-1
1989	10	250	163	91	42	155	295	188	91	37	25	-4
1989	11	225	234	100	18	116	294	250	145	2	-11	-60
1989	12	224	201	52	-4	54	248	155	49	-64	-94	-167
1990	1	124	106	64	41	130	305	316	244	42	31	14
1990	2	136	81	28	5	55	167	147	100	34	33	24
1990	3	144	86	40	20	82	191	181	127	39	35	16
1990	4	162	139	39	5	32	97	81	46	22	32	35
1990	5	117	78	22	12	51	117	58	8	-47	-53	-94
1990	6	83	24	9	14	41	80	48	9	-34	-30	-56
1990	7	51	25	15	42	67	54	9	0	-35	-54	-153
1990	8	84	68	40	69	83	62	24	6	-24	-19	-41
1990	9	146	133	55	95	124	87	20	3	-31	-30	-56
1990	10	325	253	107	169	200	193	128	74	1	6	-47
1990	11	167	169	86	146	195	259	270	226	40	50	-17
1990	12	136	114	51	100	169	247	237	163	15	28	5
1991	1	193	177	61	100	176	273	267	175	8	11	-39
1991	2	219.5	188	55.5	72.5	119.5	187.5	185.5	126.5	11.5	12	-23.5
1991	3	246	199	50	45	63	102	104	78	15	13	-8
1991	4	294	249	64	62	65	53	26	11	-3	-6	-66
1991	5	197	152	34	36	31	16	2	-4	-13	4	6
1991	6	139	80	18	28	29	10	0	-8	-17	-3	-2
1991	7	207	84	64	87	85	38	3	-9	-56	-31	-39
1991	8	258	129	64	77	74	42	10	1	-2	0	-14
1991	9	217	91	33	79	121	97	40	9	-18	-8	-21
1991	10	394	166	44	113	184	159	102	68	40	37	22
1991	11	232	131	30	109	235	262	166	73	-13	-8	-15
1991	12	291	164	32	87	197	263	188	90	-10	13	0
1992	1	137	82	27	63	130	198	221	178	10	8	-32
1992	2	511	238	28	57	123	174	173	130	14	13	6
1992	3	397	194	46	59	85	85	63	38	-2	-5	-13
1992	4	514	233	59	98	143	133	73	18	-34	-27	-40
1992	5	448	190	39	69	77	29	5	1	3	25	32
1992	6	385	179	65	110	147	81	17	-2	-21	-7	-15
1992	7	244	67	22	86	128	83	19	0	0	-2	-12
1992	8	339	105	26	77	119	74	15	0	-38	-52	-72
1992	9	223	75	24	113	232	230	143	64	8	1	-40
1992	10	268	101	21	114	258	319	225	111	-18	-16	-58
1992	11	209	72	12	62	117	122	77	45	10	11	5
1992	12	179	103	26	64	126	158	108	47	-47	-68	-103
1993	1	137	82	27	63	130	198	221	178	10	8	-32
1993	2	209	105	21	46	71	94	125	129	13	-2	-34
1993	3	197	114	25	49	80	91	72	34	-6	-13	-39
1993	4	253	102	23	55	82	67	33	14	0	-2	-23

year	mo	15x77	18x74	21X74	24X74	27x74	30x74	33x74	36x74	39x77	42x77	45x77
1993	5	304	117	34	92	129	66	2	-20	-50	-22	-39
1993	6	312	113	41	88	107	39	-1	-50	-123	-78	-74
1993	7	231	61	21	85	122	71	7	-4	-23	-26	-62
1993	8	293	117	46	111	167	99	30	9	-8	-31	-63
1993	9	234	64	14	89	155	116	46	16	1	-1	-13
1993	10	215	91	17	86	163	126	55	20	1	-1	-10
1993	11	216	110	15	96	222	263	165	77	-9	-17	-53
1993	12	243	128	15	82	192	273	264	202	20	15	-23
1994	1	219	132	19	55	133	214	239	196	24	18	-13
1994	2	133	109	18	48	95	161	199	180	55	53	46
1994	3	173	118	21	49	93	106	91	66	5	5	-11
1994	4	180	119	19	57	98	81	38	9	-9	-12	-25
1994	5	80	28	40	68	104	80	15	-3	-89	-72	-68
1994	6	-29	-32	114	139	161	107	11	-12	-123	-69	-54
1994	7	59	-3	146	119	90	17	-9	-34	-21	-9	-9
1994	8	80	-5	120	157	204	174	69	19	-19	-27	-67
1994	9	155	40	146	170	206	145	36	2	-47	-29	-36
1994	10	239	41	144	155	178	169	67	27	2	19	34
1994	11	187	22	158	197	271	318	202	81	-37	-47	-101
1994	12	163	52	130	169	249	333	212	99	-24	-41	-77
1995	1	141	29	111	132	207	342	260	194	16	22	5
1995	2	150	15	80	95	127	144	125	121	21	20	14
1995	3	140	11	90	105	140	186	141	108	17	29	16
1995	4	205	30	95	110	111	77	27	3	-11	-12	-48
1995	5	99	-5	78	102	110	72	29	5	-16	-32	-70
1995	6	138	-1	126	153	168	105	12	-11	-78	-25	-21
1995	7	266	24	141	159	150	80	6	-10	-50	16	40
1995	8	279	31	121	129	150	93	10	-5	-33	-7	-2
1995	9	292	33	129	174	216	177	88	59	1	5	-13
1995	10	393	55	156	207	257	262	140	61	-9	-6	-13
1995	11	499	109	109	146	199	247	218	190	41	53	42
1995	12	238	39	75	105	129	197	207	213	15	12	-9
1996	1	356	81	82	113	146	224	216	191	30	45	49
1996	2	321	174	88	122	157	225	225	179	21	31	29
1996	3	338	138	71	97	110	131	108	84	7	4	-27
1996	4	379	127	82	113	139	119	48	13	-9	-28	-73
1996	5	313	95	108	133	143	94	34	4	-19	-42	-88
1996	6	305	85	48	46	30	2	-6	-7	-5	-3	-7
1996	7	390	153	64	71	56	5	-6	-26	-28	-24	-25
1996	8	504	209	82	97	83	27	-1	-18	-58	-41	-48
1996	9	772	333	109	174	232	169	82	45	8	8	-22
1996	10	915	352	141	218	305	291	155	78	-4	-10	-28
1996	11	552	153	88	147	231	359	253	133	-25	-57	-110
1996	12	577	149	74	115	179	284	237	159	18	22	18
1997	1	487	85	63	94	147	216	166	115	-16	-35	-93
1997	2	458	131	75	98	132	200	232	238	57	30	25
1997	3	484	142	48	64	82	93	85	79	30	21	11
1997	4	162	1	62	67	94	129	84	34	-25	-24	-35
1997	5	160	-26	62	32	25	5	-4	-36	-33	-21	-26
1997	6	145	-102	91	52	38	7	-3	-44	-52	-25	-26

year	mo	15x77	18x74	21X74	24X74	27x74	30x74	33x74	36x74	39x77	42x77	45x77
1997	7	457	42	119	106	102	77	19	-3	-58	-43	-34
1997	8	234	-18	101	95	123	107	42	7	-6	-4	-11
1997	9	358	36	112	112	118	95	33	13	26	40	30
1997	10	468	105	127	137	162	153	43	8	-20	-19	-22
1997	11	383	32	111	127	176	213	128	51	-12	-11	-26
1997	12	593	162	106	135	164	233	207	141	26	39	37
1998	1	484	98	132	178	237	321	278	225	22	12	-4
1998	2	440	166	126	122	118	102	81	107	73	67	69
1998	3	355	84	139	149	163	187	142	97	10	4	-21
1998	4	274	8	118	91	74	49	20	5	1	0	-3
1998	5	46	-23	109	66	47	7	-5	-48	-80	-89	-86
1998	6	64	-17	69	46	54	29	1	-18	-66	-68	-74
1998	7	483	201	99	140	160	126	45	15	-44	-61	-103
1998	8	724	376	131	183	230	226	108	46	1	8	-30
1998	9	607	313	103	154	196	186	94	63	35	25	8
1998	10	333	104	74	123	211	336	315	228	21	-1	-60
1998	11	400	215	94	144	233	355	302	238	42	31	-3
1998	12	476	303	52	109	194	346	366	336	37	23	-6
1999	1	635	400	67	87	114	172	203	276	108	45	11
1999	2	220	127	29	63	101	201	188	201	39	22	-4
1999	3	430	235	64	109	133	166	116	76	27	23	14
1999	4	509	276	65	82	104	102	51	26	30	10	-16
1999	5	486	286	65	80	86	60	14	3	-1	-13	-63
1999	6	230	78	43	44	38	10	-3	-28	-21	-33	-84
1999	7	496	132	108	139	143	96	21	0	-27	-56	-103
1999	8	329	111	51	82	92	55	2	-20	-66	-70	-81
1999	9	492	185	64	129	167	167	59	14	-25	-11	-21
1999	10	737	284	41	66	86	100	51	32	17	7	-8
1999	11	578	205	60	129	206	226	136	91	5	-13	-67
1999	12	700	233	38	121	216	257	195	180	21	8	-19
2000	1	642	208	42	127	228	325	252	237	13	1	-29
2000	2	743	413	50	121	194	227	137	122	18	20	1
2000	3	492	245	47	104	169	243	187	176	24	13	-26
2000	4	366	156	46	74	103	95	45	28	11	3	-28
2000	5	364	156	33	56	54	22	1	-5	-7	-13	-26
2000	6	357	164	47	50	30	2	-61	-184	-109	-59	-58
2000	7	300	102	50	110	157	147	56	9	-12	-19	-52
2000	8	338	143	32	55	66	32	0	-10	-7	-1	8
2000	9	436	151	40	84	100	59	6	-2	-16	-14	-3
2000	10	580	287	53	117	199	205	98	55	25	19	-2
2000	11	681	297	37	106	210	315	228	134	0	-13	-39
2000	12	603	257	46	119	234	350	308	275	17	4	-32

RECENT TECHNICAL MEMORANDUMS

Copies of this and other NOAA Technical Memorandums are available from the National Technical Information Service, 5285 Port Royal Road, Springfield, VA 22167. Paper copies vary in price. Microfiche copies cost $9.00. Recent issues of NOAA Technical Memorandums from the NMFS Southwest Fisheries Science Center are listed below:

NOAA-TM-NMFS-SWFSC-306 Age validation of the first, second, and third annulus from the dorsal fin rays of lingcod (Ophiodon elongatus).
T.E. LAIDIG, K.R. SILBERBERG, and P.B. ADAMS
(June 2001)

307 Report of oceanographic studies conducted during the 1998 eastern tropical Pacific ocean survey on the research vessels *David Starr Jordan*, *McArthur*, and *Endeavor*.
V.A. PHILBRICK, P.C. FIEDLER, J.T. FLUTY, and S.B. REILLY
(July 2001)

308 Report of oceanographic studies conducted during the 1999 eastern tropical Pacific ocean survey on the research vessels *David Starr Jordan* and *McArthur*.
V.A. PHILBRICK, P.C. FIEDLER, J.T. FLUTY, and S.B. REILLY
(July 2001)

309 Report of oceanographic studies conducted during the 2000 eastern tropical Pacific ocean survey on the research vessels *David Starr Jordan* and *McArthur*.
V.A. PHILBRICK, P.C. FIEDLER, J.T. FLUTY, and S.B. REILLY
(July 2001)

310 The Hawaiian Monk Seal in the Northwestern Hawaiian Islands, 1999.
T.C. JOHANOS and J.D. BAKER
(September 2001)

311 Ichthyoplankton and station data for California Cooperative Oceanic Fisheries Investigations survey cruises in 1999.
D.A. AMBROSE, R.L. CHARTER, and H.G. MOSER
(September 2001)

312 Ichthyoplankton and station data for California Cooperative Oceanic Fisheries Investigations survey cruises in 2000.
W. WATSON, R.L. CHARTER, and H.G. MOSER
(September 2001)

313 Ichthyoplankton and station data for Manta (surface) tows taken on California Cooperative Oceanic Fisheries Investigations Survey Cruises in 1977 and 1978.
H.G. MOSER, R.L. CHARTER, D.A. AMBROSE, and E.M. SANDKNOP
(September 2001)

314 AMLR 2000/2001 field season report: Objectives, accomplishments, and tentative conclusions.
J.D. LIPSKY, Editor
(September 2001)

315 The physical oceanography off the central California coast during May-June, 1999: A summary of CTD data from pelagic juvenile rockfish surveys.
K.M. SAKUMA, F.B. SCHWING, M.H. PICKETT, D. ROBERTS, and S. RALSTON
(September 2001)